RECENT NASA METEOROID PENETRATION RESULTS FROM SATELLITES

By

Charles T. D'Aiutolo,* William H. Kinard,** and Robert J. Naumann***

ABSTRACT

The need for direct measurements in the space environment to determine meteoroid penetration rates for application to spacecraft design is discussed. Recent penetration measurements by the Explorer XVI and the Explorer XXIII satellites and the Pegasus series of satellites are presented. The primary experiment on the Explorer satellites utilized thin wall pressurized cells. These cells covering an aggregate area of about 2 square meters on each spacecraft gave indication of meteoroid puncture by loss of internal gas pressure. Each of the large winged Pegasus satellites measured meteoroid penetrations over a surface area of more than 200 square meters using electrical capacitor-type detectors which discharge when penetrated. The large detector area on these spacecraft permitted the use of target materials up to .040 cm in thickness. The penetration statistics obtained to date from the satellites are presented and compared with estimates of expected penetration rates.

The satellite measurements appear to have significantly narrowed the uncertainty in predicting the penetration frequency in materials approaching actual spacecraft skin thicknesses. Further measurements are required, however, before an accurate mass-frequency distribution of penetrating meteoroids can be established.

* NASA Headquarters, Washington, D. C.
** NASA Langley Research Center, Hampton, Virginia
*** NASA Marshall Space Flight Center, Huntsville, Alabama

RECENT NASA METEOROID PENETRATION RESULTS FROM SATELLITES

By

Charles T. D'Aiutolo,*William H. Kinard,**and Robert J. Naumann***

One of the principal parameters to be considered in the design of space vehicles is the possibility of damage resulting from impacts with extraterrestrial debris. Depending upon their kinetic energy, the impingement of high-velocity particles on spacecraft structures may result in surface erosion, puncture, or catastrophic rupture of sensitive spacecraft structures.

The problem of the spacecraft designer is to provide protection for vital parts of the spacecraft and for the occupants, if any. For this purpose he must be able to estimate the likelihood of damage, in flight, of structures of various configurations and materials.

Early knowledge of the hazard resulting from the meteoroid environment was based on information obtained from two broad fields of inquiry - astronomy, the foremost source of information, and laboratory hypervelocity impact studies. Combined information from these two sources was used to estimate the magnitude and character of the meteoroid hazard to spacecraft.

Two early estimates of the meteoroid penetration frequency, based on data from these sources, are shown in Figure 1. The estimated number of penetrations per square meter-day is plotted as a function of thickness for the penetration of aluminum sheets. The upper curve

* NASA Headquarters, Washington, D.C.
** NASA Langley Research Center, Hampton, Virginia
*** NASA Marshall Space Flight Center, Huntsville, Alabama

combined an early estimate by Professor Whipple (1958) of the meteoroid flux with a penetration criteria determined experimentally by Charters and Summers (1959) at the Ames Research Center and represented a pessimistic limit for the hazard. The lower curve combining Watson's (1956) estimate of the meteoroid flux with a theoretical penetration criteria derived by Bjork (1961) represented an optimistic limit for the hazard. For a given material thickness, an uncertainty of over three orders of magnitude existed in the estimated penetration frequency. To illustrate what such an uncertainty means in the design of space vehicles an example will be cited. In design studies for one particular spacecraft, using the upper curve of Figure 1, it was found that for adequate meteoroid protection an additional weight of about 12,500 pounds would be required. This weight would entail a severe performance penalty. Use of the lower curve resulted in no additional weight for meteoroid protection. The dilemma of the designer is readily apparent.

In order to narrow the uncertainties that have existed in predicting the probabilities of meteoroid penetrations in spacecraft structures, the Office of Advanced Research and Technology of the National Aeronautics and Space Administration has formulated a comprehensive program of investigation which includes flight experiments to measure meteoroid penetrations over a range of material thicknesses in the near-earth environment.

This paper will summarize the results to date from two series of spacecraft in this program. First, the results from the Explorer XVI and Explorer XXIII satellites, each of which exposed to the meteoroid environment a total area of about 2.0 square meters of very thin materials and used pressurized cells as the prime experiment, will be presented.

Next, preliminary results from the large satellites, Pegasus I and II, each of which exposed more than 200 square meters of material thicknesses up to 0.040 cm., using electrical capacitor-type detectors which discharge when penetrated, will be described. Finally, a comparison of the preliminary results from these satellite penetration measurements with the latest estimates based on observations of meteors will be made.

SPACECRAFT and EXPERIMENTS

Explorer XVI

Spacecraft - Two Explorer series micrometeoroid satellites have been launched to date with the primary objective of each to obtain meteoroid penetration rates in relatively thin target materials. The first of these two satellites, designated Explorer XVI (1962 Beta Chi 1) was launched December 16, 1962, from the NASA Wallops Station onboard a Scout launch vehicle. It was placed in an earth orbit having an apogee of 1180 kilometers, a perigee of 750 kilometers, and an inclination to the earth's equator of 52^{o}. The weight of the spacecraft, including the spent last-stage rocket motor which remained as part of the orbiting satellite was 233 pounds (106 kilograms).

Explorer XVI continued to transmit useful data for approximately seven and one-half months, failing on July 22, 1963. Several NASA Technical Memorandums (Hastings - 1963, 1964) have been published to date describing this satellite and the data it obtained. The data have also been presented at various other symposia (D'Aiutolo - 1964, 1964a).

Figure 2 is a photograph of the Explorer XVI spacecraft. It is cylindrical in shape, 58.5 cm. in diameter, and 193 cm. long. The primary

penetration detectors onboard consisted of pressurized cells mounted around the periphery of the last stage rocket motor.

Other penetration-type detectors placed on the spacecraft were stainless steel covered grid detectors mounted in a ring just aft of the pressure cells, copper wire card detectors mounted in a ring just aft of the steel-covered grid detectors, and two cadmium sulfide cell detectors mounted on the spacecraft nose section. Sounding-board type impact detectors were also mounted on the spacecraft nose section.

Experiments - Figure 3 is a drawing of the pressurized cell type penetration detector. The cell consists of a thin exposed surface in which penetrations are detected, a base plate, a pressure sensitive capsule, and a microswitch. Each cell, which is approximately 5.0 cm. in diameter and 18.8 cm. long, is filled with helium. When the cell is punctured, the gas leaks out and the resulting pressure loss actuates the switch that signals the telemeter of the penetration. Each cell can only detect one penetration. Beryllium copper was selected as the cell material because of previous experience in fabricating pressure diaphragms.

At the time Explorer XVI was launched, no direct measurements of meteoroid penetration rates existed, and as shown previously, estimates of expected rates varied by orders of magnitude. To insure that some useful penetration data would be obtained, the number of cells of each thickness was varied inversely as the cell skin thickness. The exact cell distribution and thickness was as follows: 100 - 0.0025 cm. cells for a total exposed area of 1.0 square meters, 40 - 0.0051 cm. cells

for a total exposed area of 0.4 square meters, and 20 - 0.0127 cm. cells for a total exposed area of 0.20 square meters.

The stainless steel covered grid detector (Davidson and Winslow, 1964) is shown in Figure 4. These detectors were made in trianglular segments with each side being about 11.6 cm. long. The stainless steel covers were 0.0025, 0.0076, and 0.0152 cm. thick. They were bonded to 12.7μ mylar which has a thin continuous grid circuit. A break in this continuous grid indicates when the stainless steel cover plate is penetrated. The area distribution for these detectors is as follows: 0.14 square meters of 0.0025 cm., 0.19 square meters of 0.0076 cm., and 0.023 square meters of 0.0152 cm.

Explorer XXIII

Spacecraft = The primary mission of the second explorer meteoroid satellite, Explorer XXIII (1964 - 74a) was to better define the penetration flux in the 0.0051 cm. material and obtain additional data in 0.0025 cm. material, thus establishing at a higher confidence level the slope of the penetration flux curve in the region of 0.0025 cm. and 0.0051 cm. thick materials. This spacecraft was launched on November 6, 1964, from the NASA Wallops Station onboard a Scout launch vehicle. It was placed in an earth orbit having an apogee of 979 kilometers, a perigee of 464 kilometers, and an inclination to the earth's equator of 52^{o}. The weight of the spacecraft, including the spent last-stage rocket motor which remained as part of the orbiting satellite, was 296 pounds (135 kilograms).

A photograph of Explorer XXIII is shown in Figure 5. It is basically very similar to Explorer XVI. The primary penetration detectors were the pressurized-cell type detector which was flown on Explorer XVI:

however, the Explorer XXIII detectors were made of stainless steel rather than beryllium copper. Since fabrication techniques had advanced to allow stainless steel to be used, this material was selected because it is a more typical spacecraft structural material.

Explorer XXIII has 70 cells of 0.0025 cm. stainless for a total area of 0.69 square meters and 140 cells of 0.0051 cm. stainless for a total area of 1.38 square meters. The area thickness distribution was selected to provide approximately equal data in the 0.0025 cm. and 0.0051 cm. cells based on the penetration rate data obtained by Explorer XVI.

Explorer XXIII also has onboard two capacitor-type penetration detectors which have a combined total area of 0.073 square meters.

Experiments - The primary penetration detectors, pressurized cells, are described above.

Figure 6 shows the details of the capacitor-type detectors which are onboard. Each detector is approximately 16.8 cm. by 21.1 cm. The outer target material is 0.002 cm. stainless steel. A dielectric consisting of a bilaminate of 4μ mylar is bonded together and to the stainless steel with the thickness of each adhesive bond being approximately 0.76 microns. Approximately 0.3μ of copper are deposited on the rear surface of the dielectric to serve as the rear capacitor electrode.

The capacitors are charged to approximately 14 volts. The operation of the detector depends on ionization being created by the energy dissipated by a penetrating meteoroid. This ionization, which is very short-lived, provides a conducting path through which the capacitor is partially discharged. The discharging of the capacitor thus provides the signal of

the penetration event. Since the shorting mechanism is temporary, the detector can recharge and be used repeatedly for detecting meteoroid penetrations.

Pegasus I and II

Spacecraft - The primary mission of the Pegasus spacecraft is the measurement of meteoroid penetration rates in materials up to 0.040 cm. in thickness. The first spacecraft, Pegasus I (1965-09A), was launched on February 16, 1965, from Cape Kennedy onboard the SA-9, Saturn I launch vehicle. It was placed in an earth orbit having an apogee of 740 kilometers, a perigee of 495 kilometers, and an inclination to the earth's equator of 32°. The second spacecraft, Pegasus II (1965-39A), was launched from Cape Kennedy on May 25, 1965, onboard the SA-8, Saturn I launch vehicle, and was placed into almost an identical orbit having the following parameters: apogee - 745 kilometers, perigee - 510 kilometers, and inclination of 32°. A third spacecraft, Pegasus III (1965-60A), was launched on July 30, 1965, from Cape Kennedy onboard the SA-10, Saturn I launch vehicle, and placed into a near-circular earth orbit. Its parameters are: apogee - 541 kilometers, perigee - 520 kilometers, and inclination - 29°. Since at the time of this writing Pegasus III has only been in orbit a few weeks, the results obtained will not be reported herein, but will be published elsewhere at a later date when more data are available.

Each spacecraft was identical in configuration. Figure 7 is an artist's concept of the Pegasus spacecraft in orbit. During launch the spacecraft was folded and when inserted into orbit was extended in an accordion-like manner. To provide a lifetime of a least one year, the

spacecraft remained attached to the spent second stage of the launch vehicle. In the fully extended condition, the spacecraft has a span of about 29.2 meters. Exclusive of the attached spent second stage, the weight is about 3200 pounds (1455 kilograms).

Experiments - The penetration detectors onboard consist of parallel plate capacitors. The erectable winglike structure of the Pegasus spacecraft supports 208 such detectors, each of which measures 50 x 100 cm. and are attached to both sides of the wings. As shown in Figure 8, the parallel plate capacitor penetration detectors are formed by backing target sheets with a 12μ mylar trilaminate which, in turn, is backed by a vapor-deposited copper layer. The capacitors are bonded to each side of a 2.54 cm. foam core which acts as a structural support as well as a barrier to prevent the meteoroid and debris resulting from penetration of one capacitor from impinging on the opposite capacitor. An Alodine coating is placed on the target sheets for thermal control. Thicknesses of the target sheets are as follows: 40μ-1100-0 aluminum, 200μ-2024 T-3 aluminum, and 400μ-2024 T-3 aluminum. The winglike structure provides 194.5 square meters of instrumented area of which 171 square meters is allocated to the 400μ thickness, 16 square meters to the 200μ thickness, and 7.5 square meters to the 40μ thickness.

The 400μ area is subdivided into 48 identifiable logic groups, each containing 5-8 individual detector sheets; the 200μ area has 6 logic groups, each containing 3-8 individual detectors; the 40μ area has 8 logic groups, each with 2 detectors. Figure 9 shows the

location of the various panel logic groups. The notation on this figure is as follows: The number without a letter represents the 400μ thickness; the letter B represents the 200μ thickness; and the letter C represents the 40μ thickness.

A penetration through the detector target sheet and mylar dielectric momentarily shorts the capacitor detector which is normally maintained at a 40-V potential by a network of current recharge amplifiers (CRA). The energy stored in the capacitor is dumped into the shorted area, which burns away the Cu vapor deposit and clears the detector in approximately 1 sec. The initial voltage drop across the capacitor starts an integrator in the hit detector which integrates the voltage variation across the detector panel for 250μ-sec. If the integrated voltage-time product is greater than a certain predetermined value, a hit word is written in the memory and a cumulative counter is incremented.

The recharge of the panel is accomplished by 3 CRA's which are selected by a diode-resistor logic matrix in a unique pattern for each logic group. This pattern also is written into the hit word.

In laboratory testing of the detectors, it was found that the discharge voltage produced by a high-velocity particle ranges from fractions of volts to full discharge. No direct correlation between discharge level, and any projectile property could be found, although there was some indication that the signal levels increased somewhat at higher velocities. The voltage-time product required to record a hit word was selected so that a typical discharge of 4 volts would be registered on

Pegasus II and III, 3 volts on the 40 mil panels on Pegasus I, and 5 volts on the remainder of the Pegasus I panels. Laboratory tests indicate that these settings would accept 80 to 90% of the signals resulting from meteoroid penetrations.

RATE OF METEOROID PENETRATIONS

Explorer XVI

Accumulative Penetrations - Explorer XVI has provided the first significant data on the penetrating capability of meteoroids in thin structural materials. Figure 10 shows the accumulated punctures as a function of time for the 0.0025 cm. and 0.0051 cm. beryllium-copper pressurized cells as well as the 0.0025 cm. and 0.0076 cm. stainless steel covered grid detectors. The data presented extend from December 16, 1962, (launch) through July 22, 1963, at which time the spacecraft ceased to transmit data. During the seven and one-half months in orbit, forty-four 0.0025 cm. beryllium-copper and eleven 0.0051 cm. beryllium-copper penetrations had been recorded. There have also been six 0.0025 cm. stainless steel and one 0.0076 cm. stainless steel penetrations recorded in this time period. As discussed by Secretan (1965), several penetrations of the cadmium-sulfide cell were recorded. Although not reported, two penetrations were recorded in copper wire card detectors. There were no penetrations recorded in either of the 0.0127 cm. beryllium-copper pressurized cells or the 0.0152 cm. stainless steel wire grid.

Penetration Rates - The penetration data that have been obtained from the pressure cells and the stainless steel covered grid detectors are

shown in Figure 11. The thickness of the detector target is plotted on the abscissa and the puncture rate is plotted on the ordinate.

Some very preliminary impact tests performed at LRC and at Ames have indicated that equal thicknesses of the stainless steel used and the beryllium copper used have approximately the same resistance to penetration.

It can be seen that a flux of 3.86×10^{-6} punctures/meter^2-sec. was observed in the 0.0025 cm. pressure cells. This flux is based on the 44 penetration events. The flux measured in the 0.0051 cm. cells is 1.99×10^{-6} punctures/meter^2-sec. based on the 11 events. As stated above, there were no penetrations observed in the 0.0127 cm. cells and the point shown in Figure 11 represents an upper limit of the flux.

The stainless steel covered detectors, due to their small exposed area, received a small number of penetrations. The six 0.0025 cm. penetrations give a flux rate of 1.329×10^{-6} punctures/meter^2-sec., while the one 0.0076 cm. penetration gives a flux rate of 8.68×10^{-7} punctures/meter^2-sec.

In summary, Explorer XVI established with a reasonable level of confidence the penetration flux in 0.0025 cm. beryllium copper and to a reduced confidence level the flux in 0.0051 cm. beryllium copper. The stainless steel data seem to agree with the beryllium results.

Explorer XXIII

Accumulative Penetrations - Presented in Figure 12 is the accumulated punctures as a function of time for the 0.0025 cm. and 0.0051 cm. stainless steel pressurized cells. The data presented extend from November 6,

1964, (launch) through July 22, 1965. In this time period, forty-three 0.0025 cm. and fifty-four 0.0051 cm. pressurized cells have been penetrated. There have also been two penetrations recorded in the capacitor detector during the same time period.

Penetration Rates - The penetration data obtained by Explorer XXIII prior to July 22, 1965, is presented in Figure 13, which is a plot of the penetration rate on the ordinate and the material thickness on the abscissa. The penetration rates for the 0.0025 cm. and 0.0051 cm. materials are 3.74×10^{-6} and 1.87×10^{-6} penetration/meter^2-sec., respectively.

As of July 22, 1965, the capacitor detectors had been penetrated only twice, and as a result, calculated penetration rates for these detectors have little statistical significance. The calculated rate for the capacitors does seem to be in reasonable agreement with the 1-mil pressure cells. The fact that the capacitor detector rate is low, compared to the pressure cell rate, could result from either or both of two factors. The first factor as already mentioned is the small data sample of only two events. The second factor which would cause the capacitor detector rates to be lower than cells results from a difference in the threshold detection for each detector. The pressure cell detectors will indicate as a penetration any impact that penetrates in the material a sufficient depth to allow small cracks to develop between the crater bottom and the rear of the plate. The actual penetration depth in these cases may be only 2/3 the thickness of the plate. The capacitor detectors, on the other hand, require a complete

penetration of the target and the dielectric forming the capacitor before an impact is detected and consequently, even though both types of detectors have 0.0025 cm. plates, the capacitor will require a little larger particle under the same impact velocities to detect a penetration.

Figure 14 compares the results of Explorer XVI and Explorer XXIII. It can be seen that the data from the beryllium-copper pressure cells of Explorer XVI fall almost on top of the data obtained by the stainless steel cells of Explorer XXIII. This fact supports the finding from ground tests which indicated that the stainless steel and beryllium-copper material used both have about the same resistance to penetrations. There is also good agreement in the data obtained from the 0.0025 cm. pressurized cells and the 0.0025 cm. stainless steel grid detector. Little significance can be placed in the 0.0076 cm. stainless steel grid data and the 0.0127 cm. beryllium-copper cell data since only one penetration was recorded in the grid detector and no penetrations were recorded in the beryllium copper cell detector.

With the large total data sample obtained by both satellites, the rates at the 0.0025 cm. and 0.0051 cm. materials based on the pressure cell measurements are established with very good confidence as evidenced by the confidence limits shown on the data points.

Pegasus I and II

Minor instrumentation difficulties in Pegasus I prevented panel identification and recharge times from being recorded for the 200 and 400 panels. Also, it was found that these panels had a tendency to become intermittent, that is a single panel may suddenly generate many

hit words in the space of a few orbits. It is believed that such a condition is caused by debris or ragged edges around a meteoroid perforation that produce point physical shorting. The energy stored in the capacitor would burn away such a short, but thermal expansion and contraction could cause the process to repeat many times. Laboratory tests to investigate this phenomenon will be conducted in the near future.

Pegasus I received four hit indications on the 400μ panels in the first 11 days. However, several panels became intermittent at that time, and the lack of panel identity precluded separating valid hits from the intermittent events after that time. Based on four events in 1925 m^2 days, the penetration frequency is .0021/m^2 days.

For Pegasus I, a very high fraction of the penetrations on the 200μ panels resulted in shorts and since there are only six logic groups, the 200μ area very quickly became lost. There were nine hit indications in 248/m^2 days exposure which resulted in a penetration frequency of .036/m^2 days. Again it should be pointed out that the 200 and 400μ hit words did not contain panel identity or recharge time unless a short resulted. Therefore, some of the tests for validity could not be made.

The 400μ panels gave panel identification about 70% of the time for Pegasus I and are still functioning extremely well. A total of 104 penetrations have been recorded in 858/m^2 days for a flux of .121/m^2 days. A time history of the cumulative events is shown in Figure 15.

The number of penetrations, area-time exposure, and puncture frequency observed by Pegasus I and II (as of July 20, 1965) are summarized

in Table I. Note that the few punctures observed in the 200μ and 400μ Pegasus I detectors are in reasonably good agreement with Pegasus II results. The total 40μ events give a somewhat higher puncture rate for Pegasus II than for Pegasus I.

One possible explanation may be seen be comparing time history of the 40μ cumulative counts on Pegasus II (Figure 16) with Figure 15. There appears to be a significant increase in counts during the periods June 6 to June 12. It is interesting to note that this period corresponds with times of known meteor shower activity, i.e., the Arietids and the γ - Perseids. Subtracting the shower events from the Pegasus II counts gives a sporadic background that is very close to the Pegasus I result. Of course, a reasonable explanation must be found for the non-observation of the showers by Pegasus I.

One plausible explanation may be found in the difference of the rotational behavior of the two satellites. Angular momentum in the form of rotation about the x-axis was imparted to both spacecraft when the residual propellants were vented. Since the x-axis is a principal axis of least moment of inertia, such a rotational state is quasi-stable for a semi-rigid body. Pegasus I underwent a transition to the minimum rotational energy state (i.e., rotation about the z-axis, which is the axis of maximum moment of inertia) in 15 days. This rotation stabilized the sensor plane in space. Gravity gradient torque causes a precession of the rotational axis which provides a relatively slow scanning of the celestial sphere.

The result of this motion may be seen in terms of the angle the sun makes with the sensor plane shown in Figure 17. Preliminary analysis

indicates that the normal to the sensor plane made angles of 50° and 65° with the radiants of the Arietids and γ - Perseids, respectively, during the times of of peak activity. Since the area presented to the shower direction is reduced by the cosine of the angle of incidence, and since the penetrating ability of an impacting meteoroid falls roughly as the 2/3 power of the cosine of the angle of incidence, it is understandable that these showers may be missed by Pegasus I. Of course, the deviation that was attributed to shower events in Pegasus II data is small and may very well be nothing more than a coincidental statistical fluctuation.

Pegasus II, for reasons that are not yet completely clear, retained its rotation about the x-axis. This rotational configuration, together with the lower angular momentum imparted to it, results in a more rapid precession of the rotational axis as is evident in Figure 18, which shows the angle between the sun and the rotational axis. The motion is such that the entire celestial sphere is swept with the sensor axis in a period of a single day. Therefore, the observation of showers having a population of detectable particles sufficiently above the sporadic background is virtually assured.

The time histories of the 200μ and 400μ cumulative counts are shown in Figures 19 and 20. The sampling rates for these thicknesses are too low to see any shower effects.

The penetration rates in the various thicknesses for Pegasus I and II are shown in relation to one another in Figure 21. The error bars indicate 95% confidence limits.

COMPARISON OF METEOROID PENETRATION RATES

The direct near-earth meteoroid penetration measurements obtained from Explorer XVI and Explorer XXIII, as well as Pegasus I and II, are compared with a current estimate (Whipple, 1963A) of the expectation of frequency of meteoroid penetrations in Figure 22. The number of penetrations per square meter-day is plotted as a function of thickness for the penetration of aluminum sheets. The .0025 cm. and .005 cm. Explorer XVI BeCu cell data, as well as the .0025 cm. and .005 Explorer XXIII stainless steel cell data, are plotted at equivalent thicknesses of aluminum based on laboratory impact tests wherein it was determined that the resistance to penetration of the beryllium copper and stainless steel is about twice that for aluminum. The bars on the satellite data indicate the statistical uncertainty in the direct measurements. With a 95% confidence, the actual value lies between the bars shown. There is reasonably good agreement between measurements obtained from the several spacecraft in spite of the fact that a number of refinements, as pointed out previously, have not yet been applied to the data. For the thinner materials, the rate of decrease of the frequency of penetration with thickness is seen to be considerably less than that previously estimated. Also, for the thin materials, there is approximately two orders of magnitude difference between the measured penetration rates and the estimate. On the other hand, the penetration frequency and rate of change in thick materials are in better agreement with the estimate.

CONCLUDING REMARKS

The direct meteoroid penetration measurements by spacecraft have significantly narrowed the uncertainty in predicting the penetration frequency in materials approaching actual spacecraft skin thicknesses. Although the data obtained are extremely useful to spacecraft designers, measurements of penetration rates in thicker materials which will correlate with ground-based observations must be determined before a complete appraisal of the near-earth meteoroid hazard to space flight can be ascertained.

REFERENCES

Bjork, B. L.
1961. Meteoroids vs. Space Vehicles. Am. Rocket Sec. J., Vol. 21, p. 803.

D'Aiutolo, C. T.
1964. Review of Meteoroid Environment Based on Results from Explorer XIII and Explorer XVI Satellites. In Space Research IV, P. Muller, ed., pp. 858-874. North-Holland Publishing Company, Amsterdam, 1964.

1964a. Satellite Measurements of the Meteoroid Environment. In Annuals of the New York Academy of Sciences, Vol. 119, Art. 1, pp. 82-97. New York Academy of Sciences, 1964.

Davison, E. H., and Winslow, P. C., Jr.
1964. Micrometeoroid Satellite (Explorer XVI) Stainless Steel Penetration Rate Experiment. NASA Technical Note D-2445, August 1964.

Hastings, E. C., et al
1963a. The Explorer XVI Micrometeoroid Satellite. Description and Preliminary Results for the Period December 16, 1962, through January 13, 1963. NASA Technical Memorandum X-810, February 1963.

1963b. The Explorer XVI Micrometeoroid Satellite. Supplement I, Preliminary Results for the Period January 14, 1963, through March 2, 1963. NASA Technical Memorandum X-824, April 1963.

1963c. The Explorer XVI Micrometeoroid Satellite. Supplement II, Preliminary Results for the Period March 3, 1963, through May 26, 1963. NASA Technical Memorandum X-899, September 1963.

1964. The Explorer XVI Micrometeoroid Satellite. Supplement III, Prelimiary Results for the Period May 27, 1963, through July 22, 1963. NASA Technical Memorandum X-949, March 1964.

Secretan, L.
1965 Measurements of Interplanetary Dust Particle Flux from Explorer XVI Cd S Dust Particle Detector. In proceedings of the Symposium on Meteor Orbits and Dust.

Summers, J. L.
1959 Investigation of High-Speed Impact: Regions of Impact and Impact at Oblique Angles. NASA Technical Note D-94, October 1959.

Watson, F. G.
1956. Between the Planets. Harvard University Press, Cambridge, Massachusetts, 1956.

Whipple, F. L.
1958. The Meteoritic Risk to Space Vehicles. In Vista in Astronautics (Vol. 1). M. Alperin, ed., pp. 115-124. Pergamon Press, London, England, 1958.

1963a. On Meteoroids and Penetration. Jour. Geophys. Res., Vol. 68, No. 17, pp. 4929-4939.

TABLE I

PEGASUS I AND II PENETRATION RATES

	NUMBER OF PENETRATIONS	AREA-TIME (M^2 DAY)	FREQUENCY OF PENETRATIONS (No. / M^2 SEC)
PEGASUS I			
400 μ	4	1925	2.4×10^{-8}
200 μ	9	248	4.2×10^{-7}
40 μ	104	858	1.4×10^{-6}
PEGASUS II			
400 μ	30	8457	4.0×10^{-8}
200 μ	14	734	2.2×10^{-7}
40 μ (TOTAL)	61	357	2.0×10^{-6}
40 μ (SHOWER PEAK)	12	26	5.3×10^{-6}
40 μ (SPORADIC)	40	299	1.5×10^{-6}

FIGURE CAPTIONS

Figure

1. Estimated Meteoroid Penetration Frequency
2. Schematic Drawing of Explorer XVI (1962 Beta Chi I) Satellite
3. Sketch of Pressurized Cell Detector
4. Sketch of Stainless Steel Covered Grid Detector
5. Schematic Drawing of Explorer XXIII (1964-74a)
6. Typical Cross-Section of Explorer XXIII Capacitor Detector
6a. Explorer XXIII Capacitor Penetration Detector
7. Pegasus Satellite Configuration with Body-Fixed Coordinate Axes Indicated
8. Pegasus Capacitor Detector
9. Pegasus Wing Panel Schematic Showing Location of Various Logic Groups
10. Explorer XVI History of Accumulated Penetrations
11. Explorer XVI Penetration Rates
12. Explorer XXIII History of Accumulative Penetrations
13. Explorer XXIII Penetration Rates
14. Comparison of Explorer XVI and Explorer XXIII Penetration Rates
15. Time History of Accumulated Penetrations for 40μ Panels on Pegasus I
16. Time History of Accumulated Penetrations for 40μ Panels on Pegasus II
17. Angle Sun Makes with Pegasus I Sensor Plane as a Function of Time
18. Angle Sun Makes with Pegasus II Rotational Axis as a Function of Time
19. Time History of Accumulated Penetrations for 200μ Panels on Pegasus II
20. Time History of Accumulated Penetrations for 400μ Panels on Pegasus II
21. Pegasus I and II Penetration Rates
22. Comparison of Meteoroid Penetration Rates

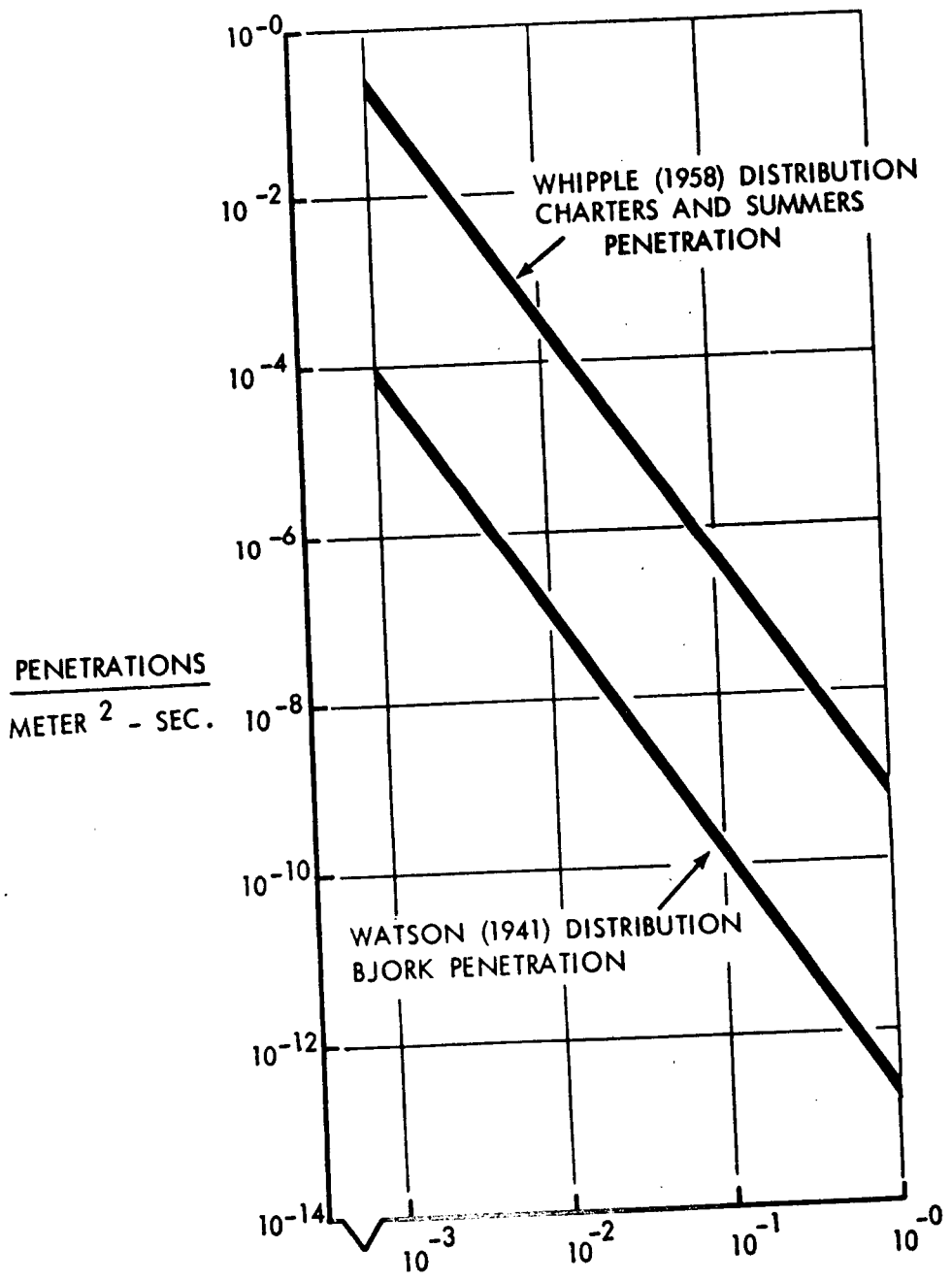
10^{-0}
10^{-2}
10^{-4}
10^{-6}
10^{-8}
10^{-10}
10^{-12}
10^{-14}
WHIPPLE (1958) DISTRIBUTION
CHARTERS AND SUMMERS
PENETRATION
WATSON (1941) DISTRIBUTION
BJORK PENETRATION
PENETRATIONS
METER ^{2} - SEC.
10^{-3}
10^{-2}
10^{-1}
10^{-0}
THICKNESS OF ALUMINUM, cm

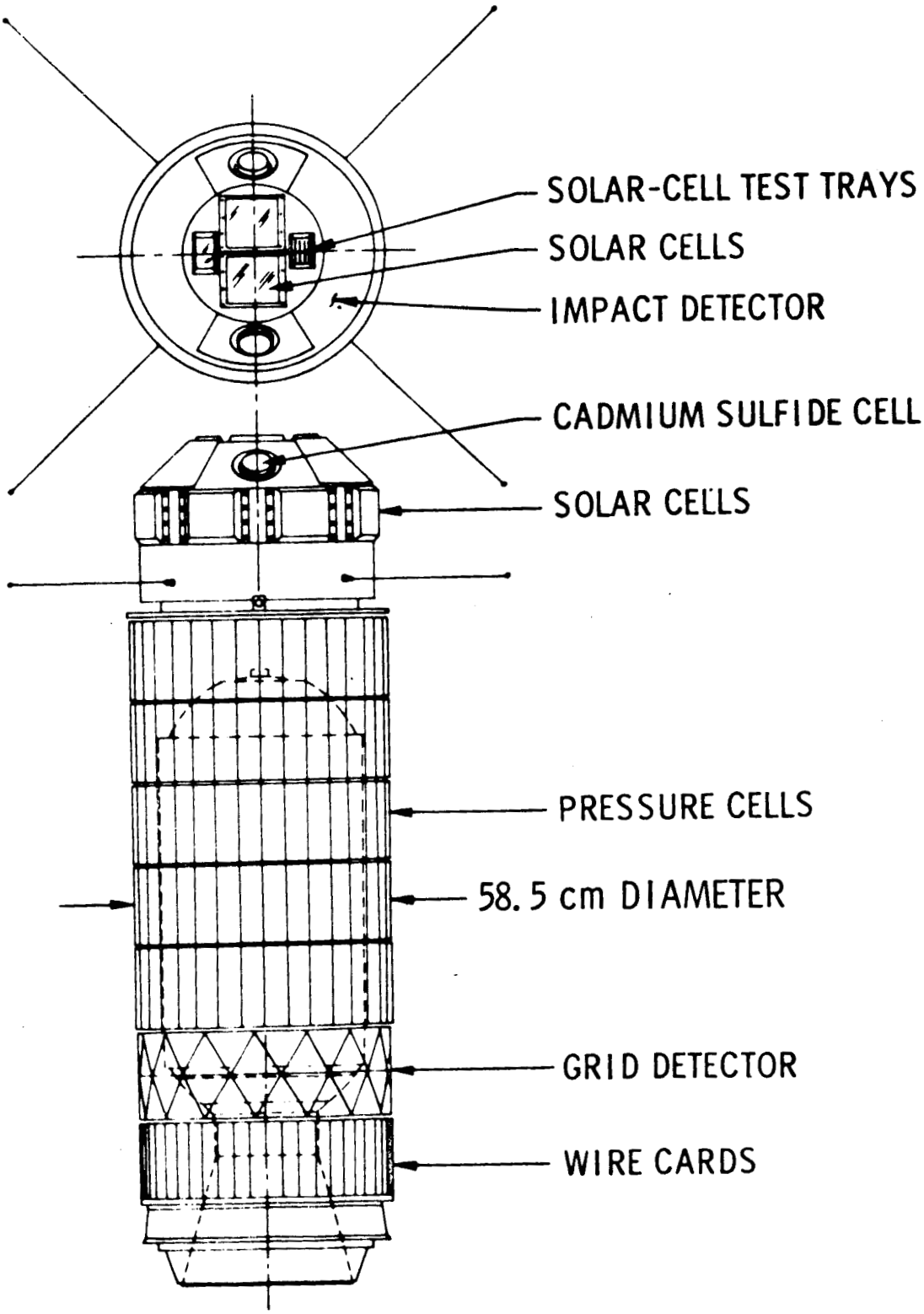
SOLAR-CELL TEST TRAYS
SOLAR CELLS
IMPACT DETECTOR
CADMIUM SULFIDE CELL
SOLAR CELLS
PRESSURE CELLS
58.5 cm DIAMETER
GRID DETECTOR
WIRE CARDS

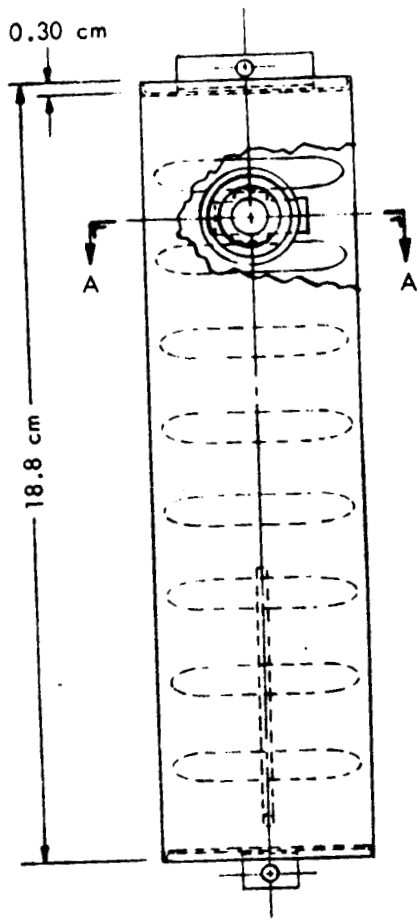
0.30 cm
A
A
18.8 cm

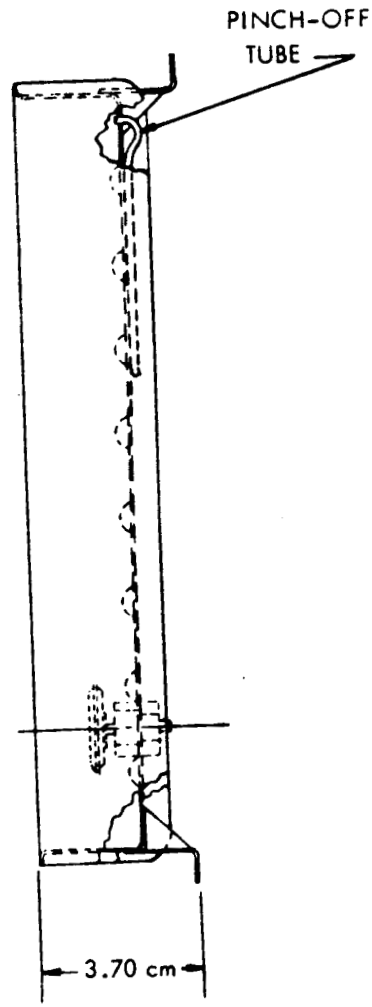
PINCH-OFF
TUBE
3.70 cm

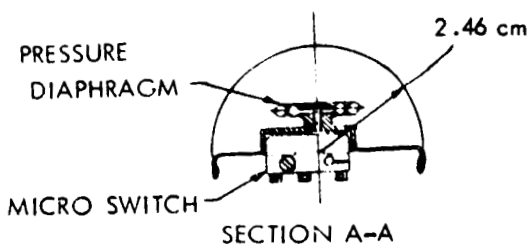
2.46 cm
PRESSURE
DIAPHRAGM
MICRO SWITCH
SECTION A-A

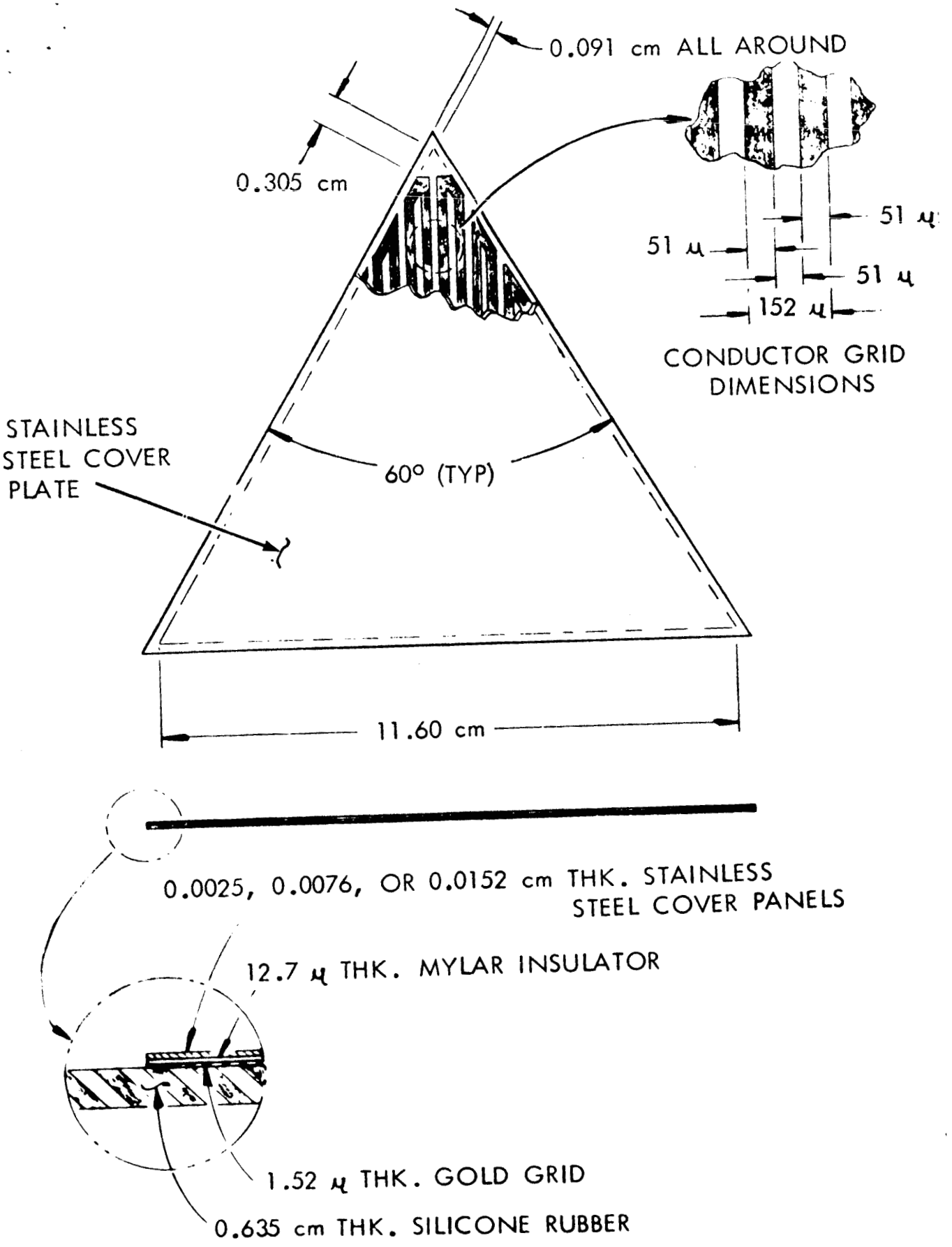
0.091 cm ALL AROUND
0.305 cm
51 μ
51 μ
51 μ
152 μ
CONDUCTOR GRID DIMENSIONS
STAINLESS STEEL COVER PLATE
60° (TYP)
11.60 cm
0.0025, 0.0076, OR 0.0152 cm THK. STAINLESS STEEL COVER PANELS
12.7 μ THK. MYLAR INSULATOR
1.52 μ THK. GOLD GRID
0.635 cm THK. SILICONE RUBBER

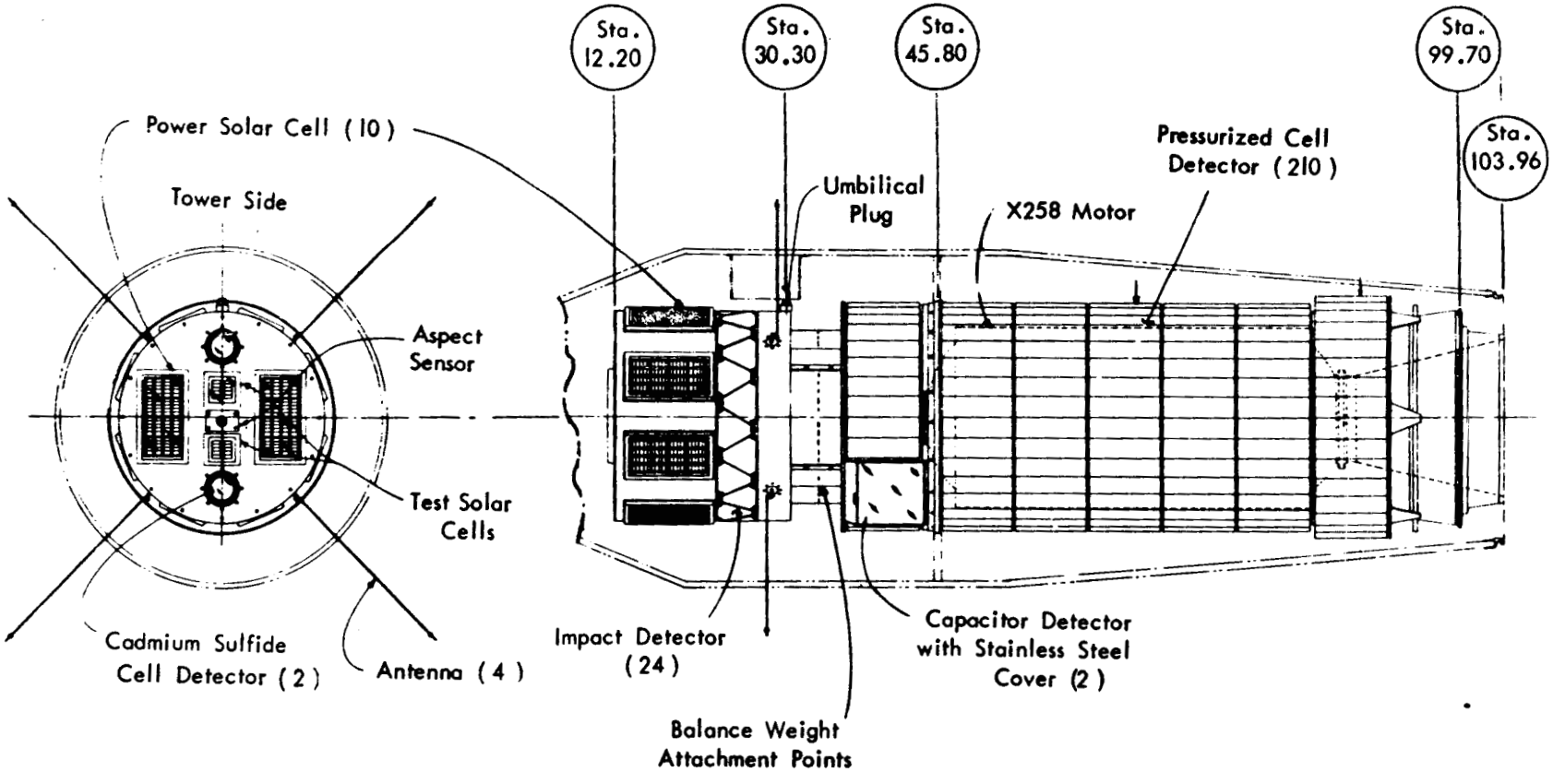
Sta. 12.20
Sta. 30.30
Sta. 45.80
Sta. 99.70
Sta. 103.96
Power Solar Cell (10)
Tower Side
Aspect Sensor
Test Solar Cells
Cadmium Sulfide Cell Detector (2)
Antenna (4)
Umbilical Plug
X258 Motor
Pressurized Cell Detector (210)
Impact Detector (24)
Balance Weight Attachment Points
Capacitor Detector with Stainless Steel Cover (2)

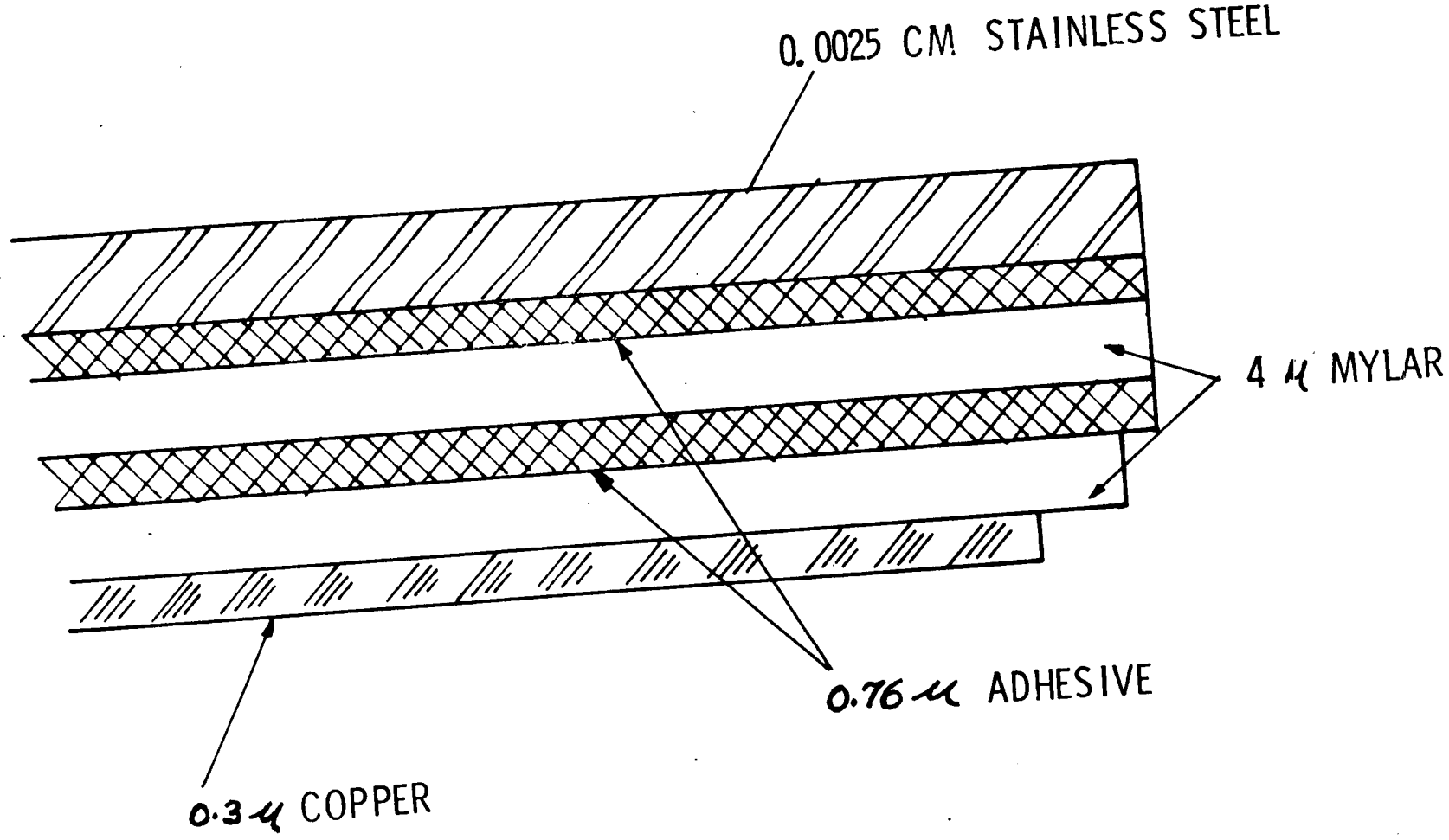
0.0025 CM STAINLESS STEEL
4 μ MYLAR
0.76 μ ADHESIVE
0.3 μ COPPER

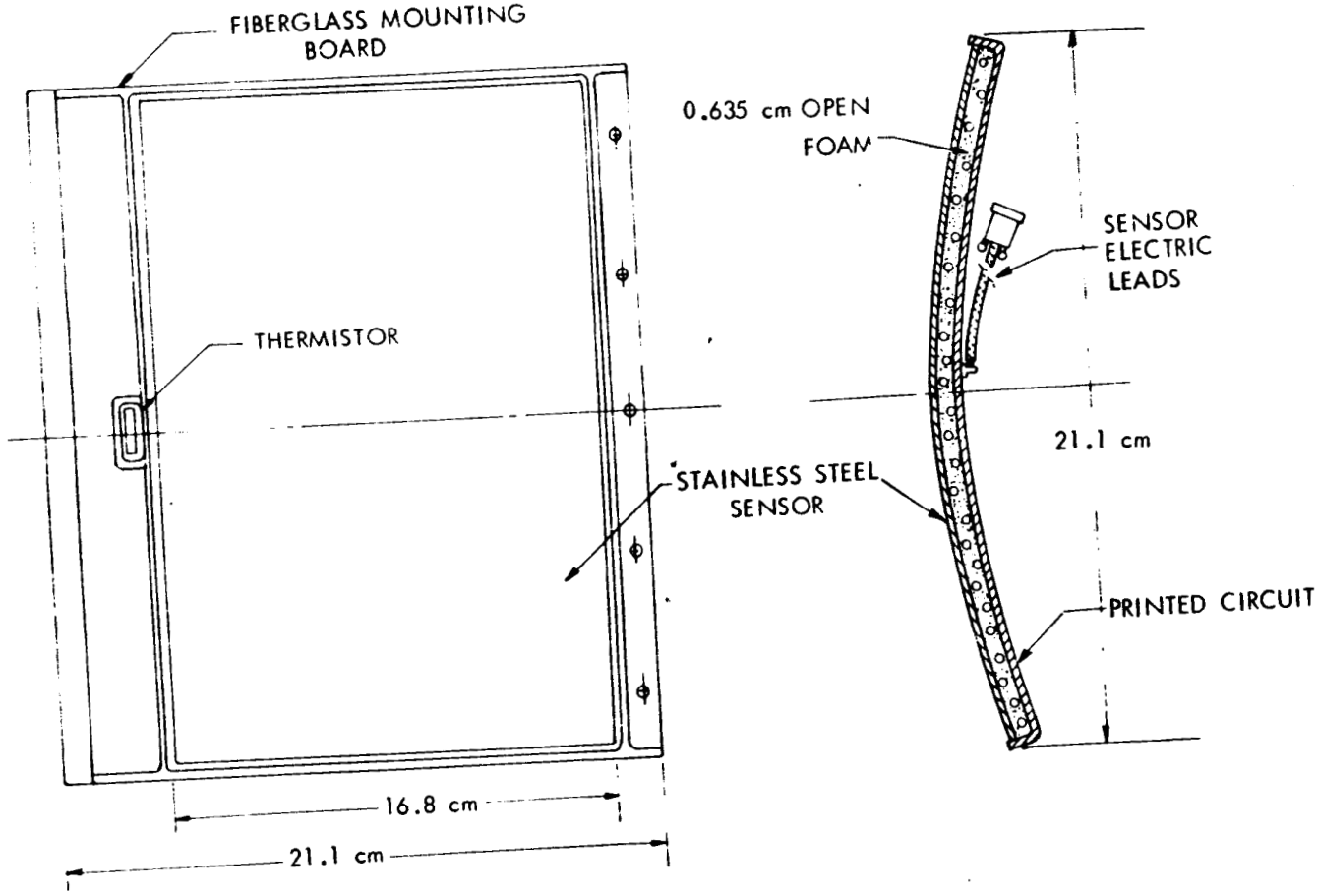
FIBERGLASS MOUNTING BOARD
THERMISTOR
16.8 cm
21.1 cm
0.635 cm OPEN FOAM
SENSOR ELECTRIC LEADS
21.1 cm
STAINLESS STEEL SENSOR
PRINTED CIRCUIT

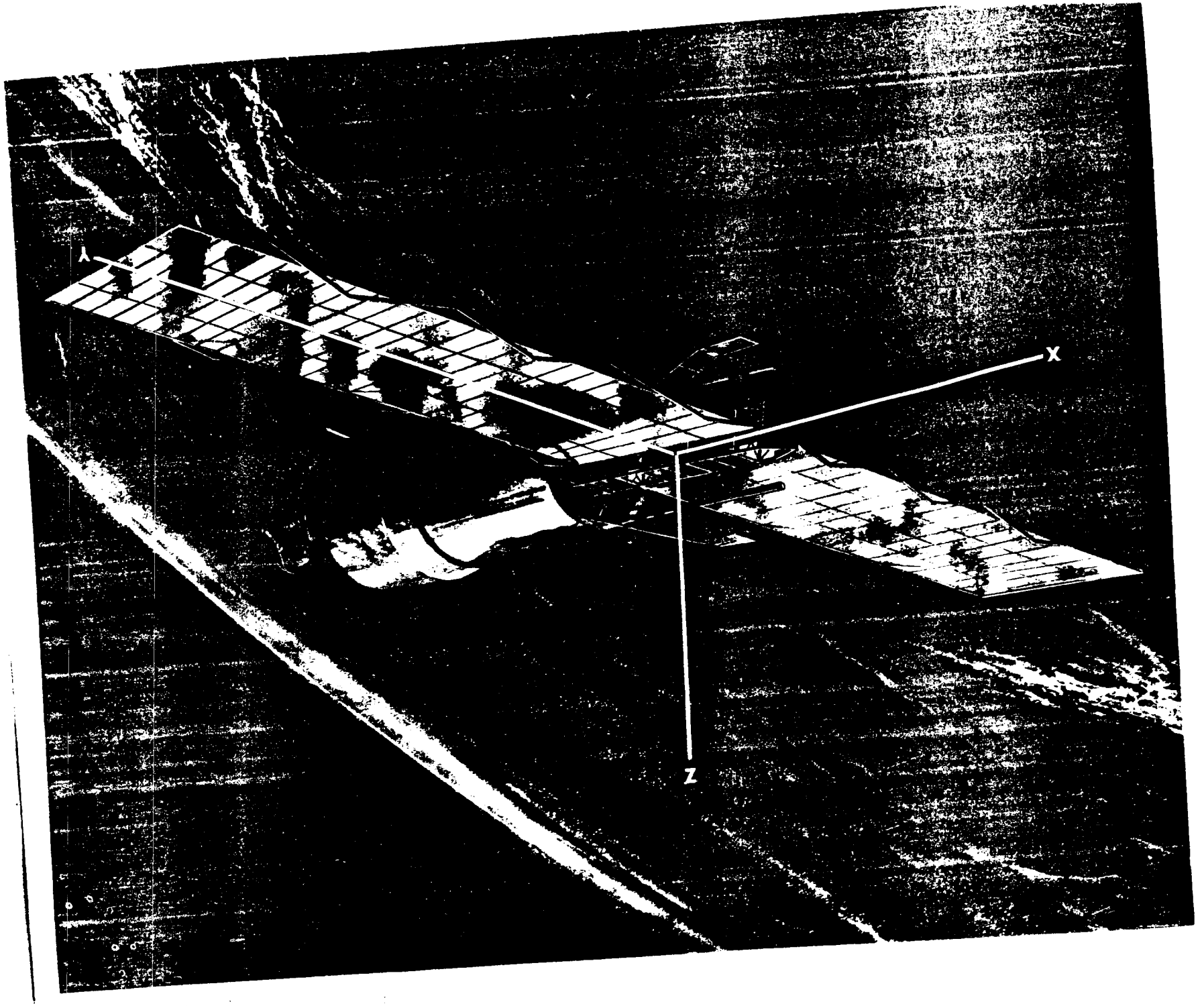
Y
X
Z

METEOROID DETECTOR PANEL

EXPLODED VIEW

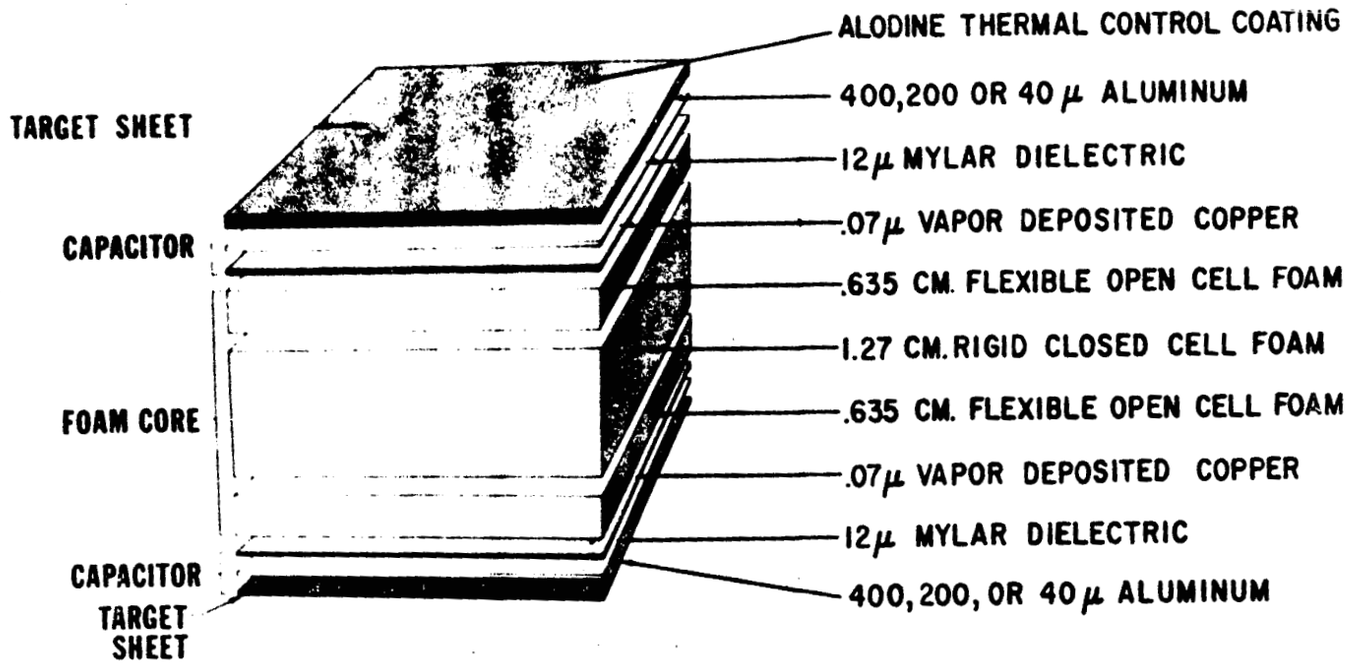

Note: The 40μ capacitors are bonded directly to 2.54 cm rigid foam cores with a 125μ layer of Rubber Asbestos Corp. M690 epoxy.

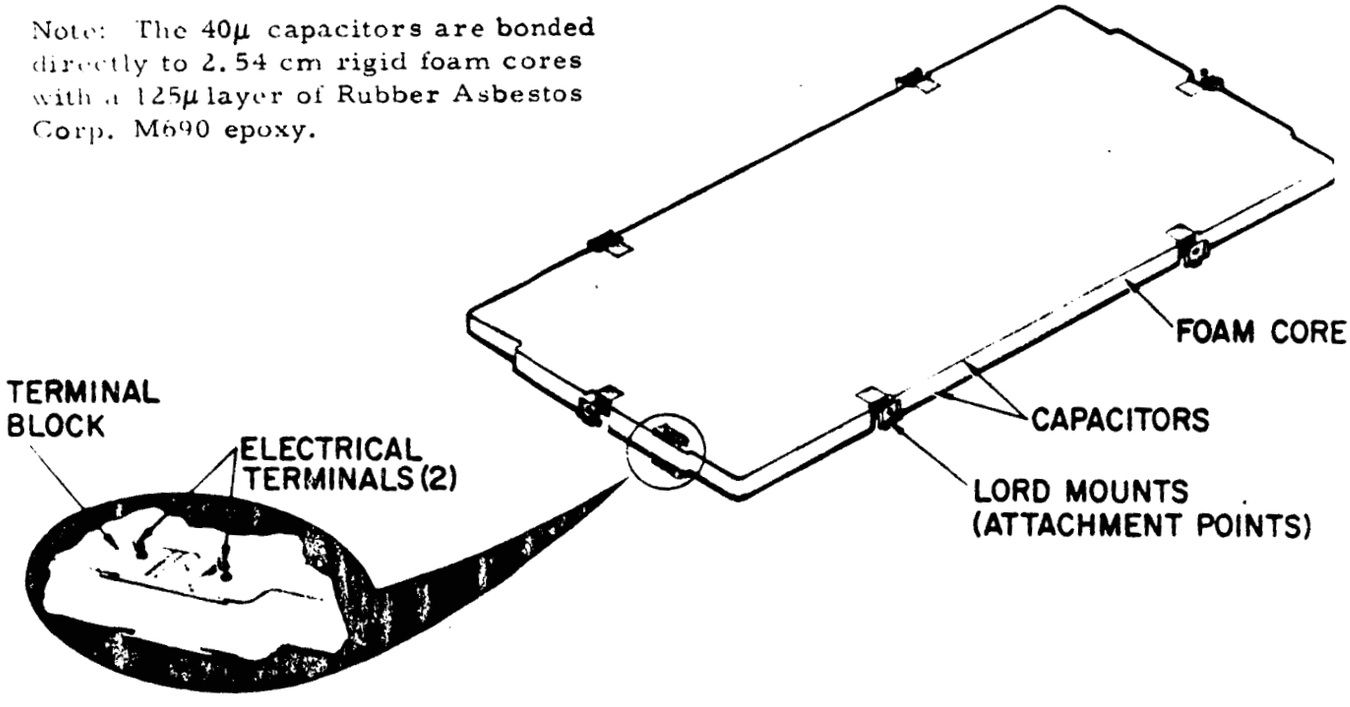

PEGASUS DETECTOR PANELS

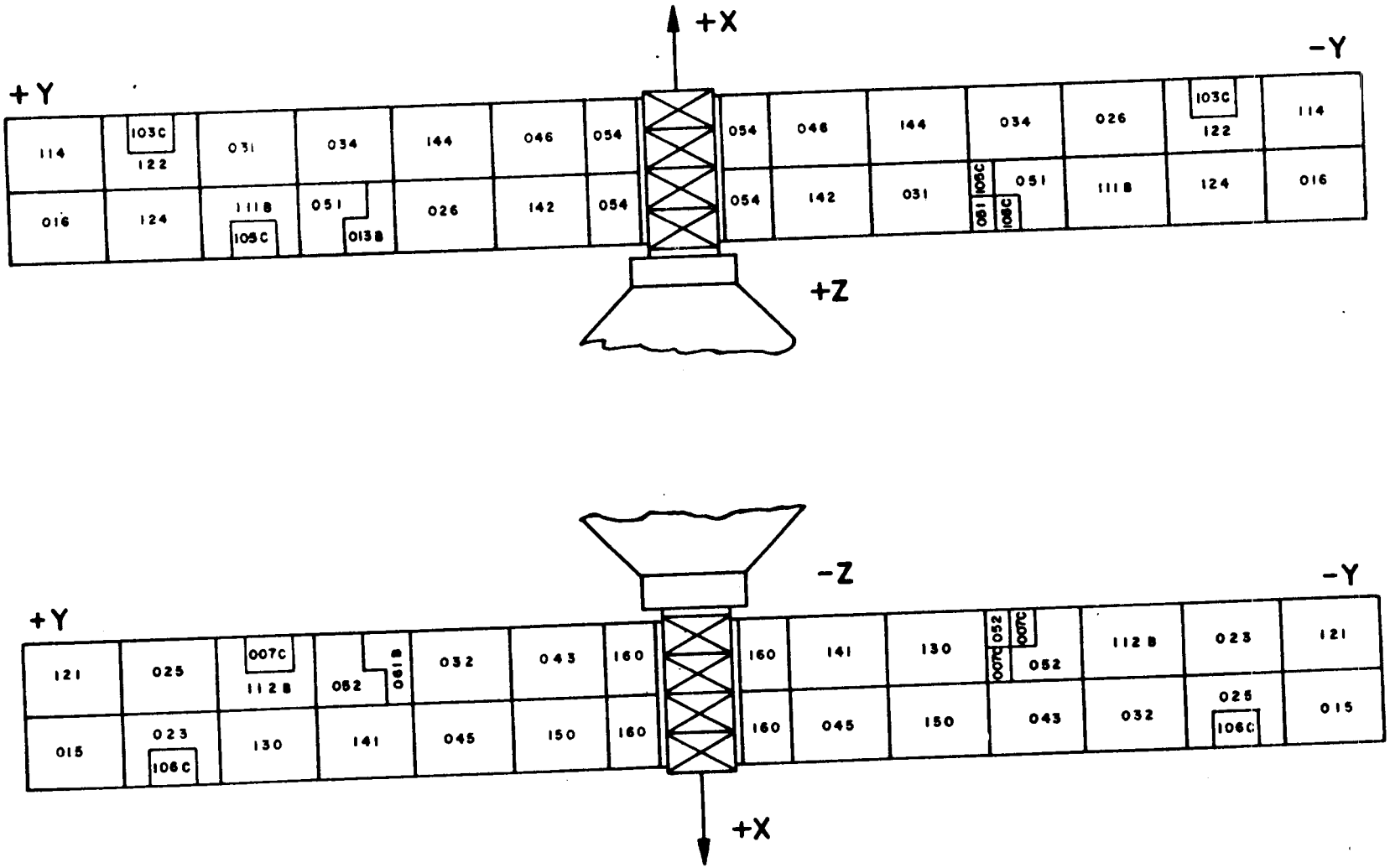

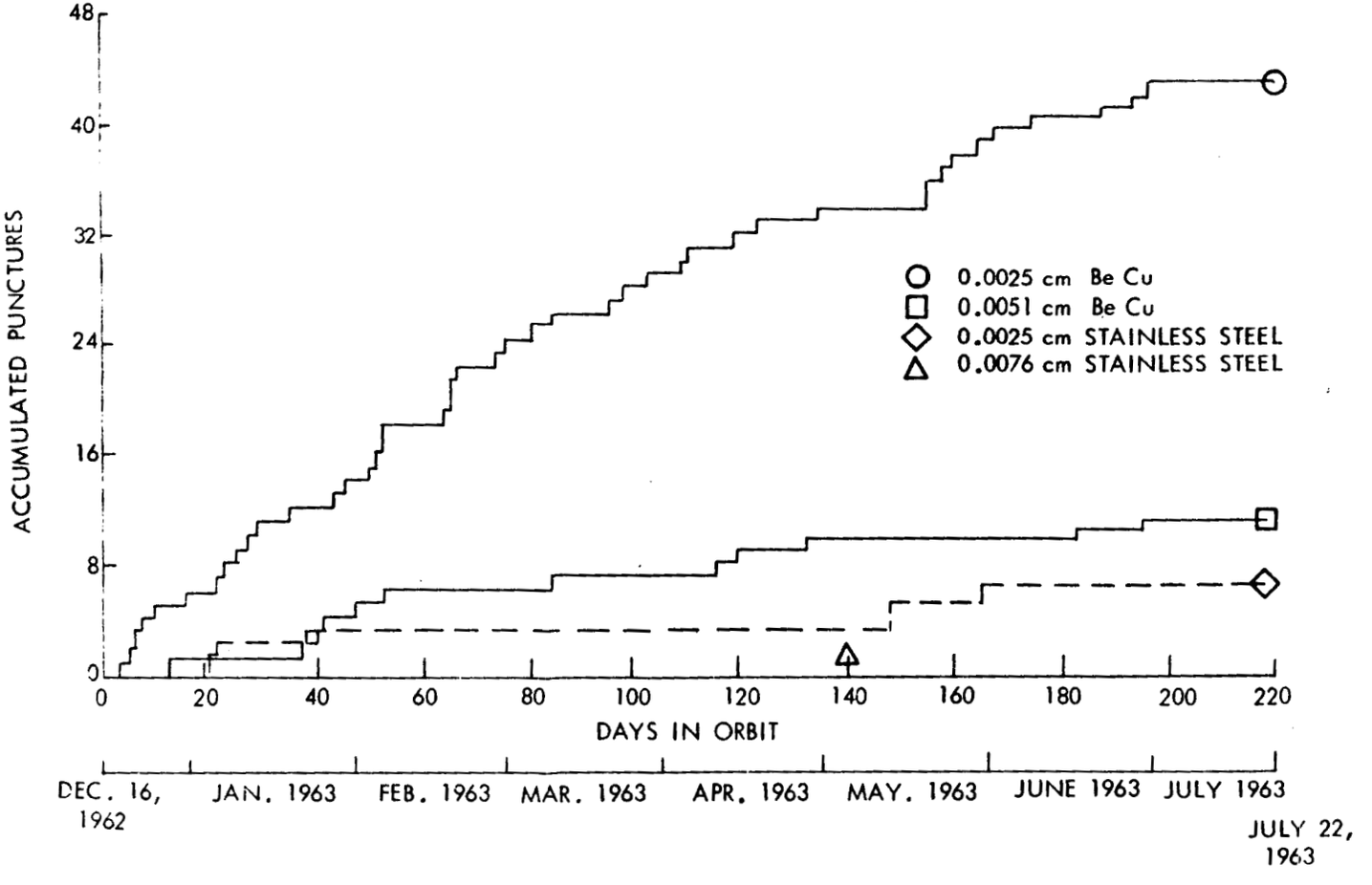
ACCUMULATED PUNCTURES
48
40
32
24
16
8
0
0.0025 cm Be Cu
0.0051 cm Be Cu
0.0025 cm STAINLESS STEEL
0.0076 cm STAINLESS STEEL
0
20
40
60
80
100
120
140
160
180
200
220
DAYS IN ORBIT
DEC. 16, 1962
JAN. 1963
FEB. 1963
MAR. 1963
APR. 1963
MAY. 1963
JUNE 1963
JULY 1963
JULY 22, 1963

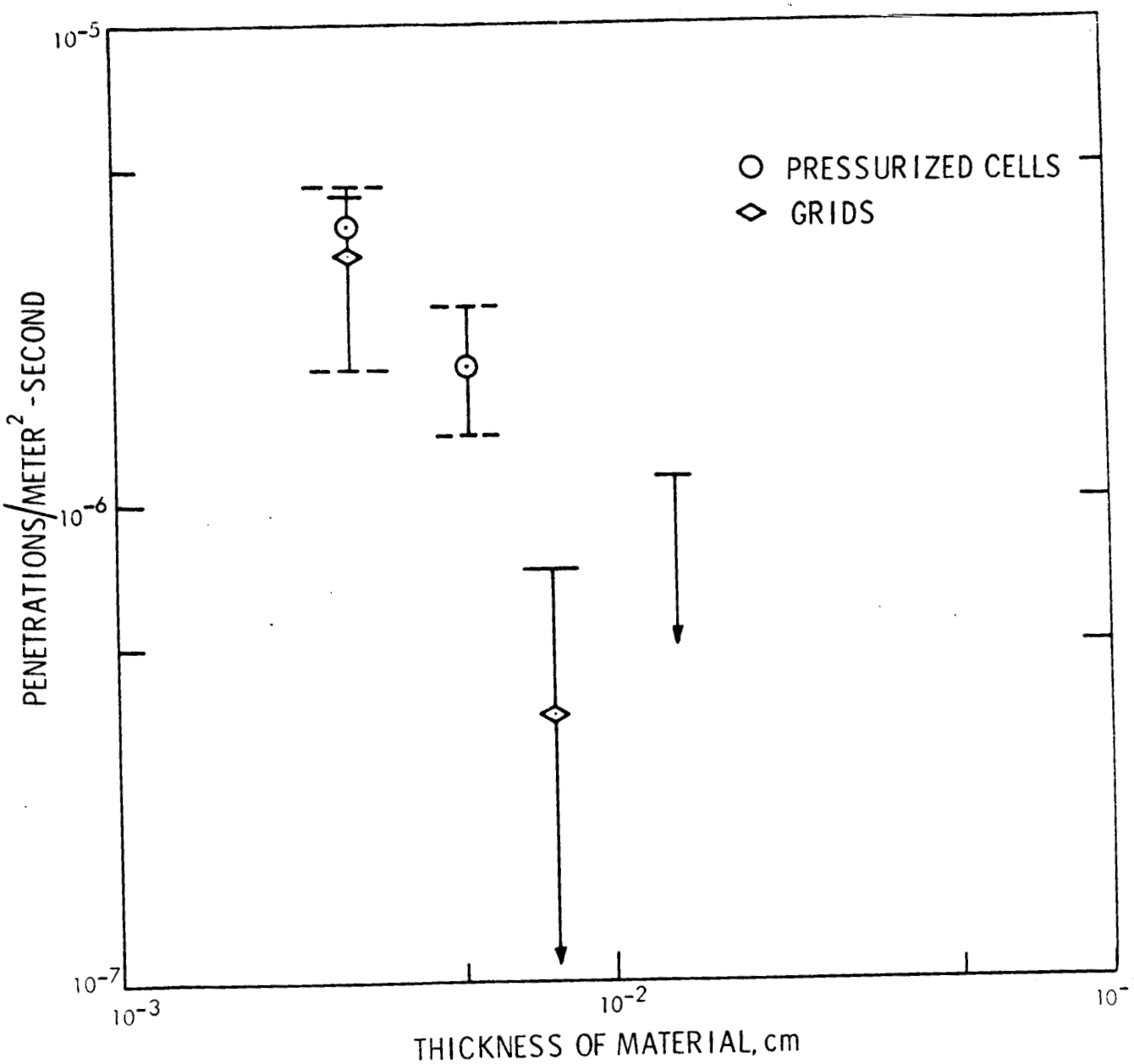
PENETRATIONS/METER^2-SECOND
10^{-5}
10^{-6}
10^{-7}
10^{-3}
10^{-2}
10^{-1}
THICKNESS OF MATERIAL, cm
PRESSURIZED CELLS
GRIDS

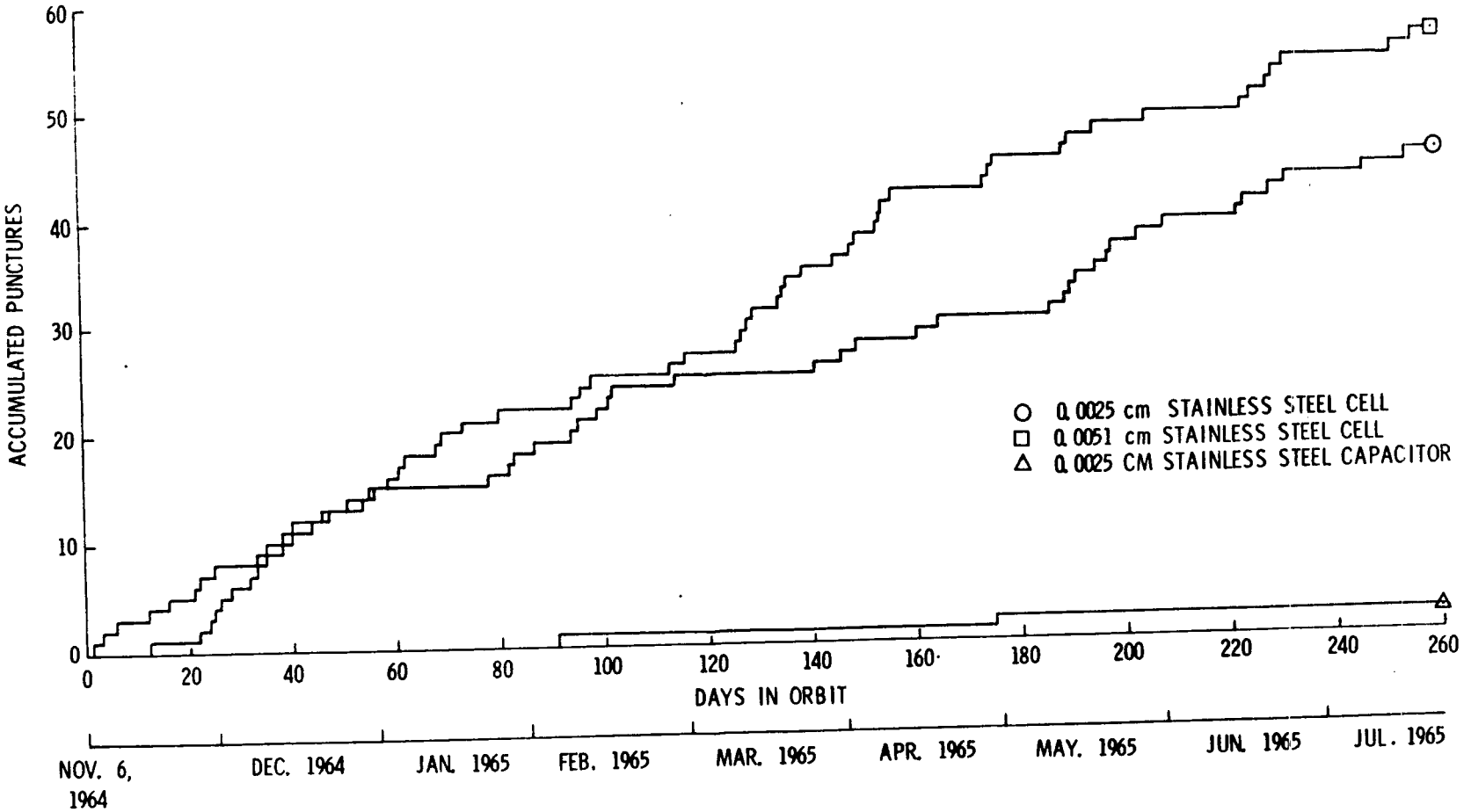
ACCUMULATED PUNCTURES
60
50
40
30
20
10
0
0
20
40
60
80
100
120
140
160
180
200
220
240
260
DAYS IN ORBIT
NOV. 6, 1964
DEC. 1964
JAN. 1965
FEB. 1965
MAR. 1965
APR. 1965
MAY. 1965
JUN. 1965
JUL. 1965
0.0025 cm STAINLESS STEEL CELL
0.0051 cm STAINLESS STEEL CELL
0.0025 CM STAINLESS STEEL CAPACITOR

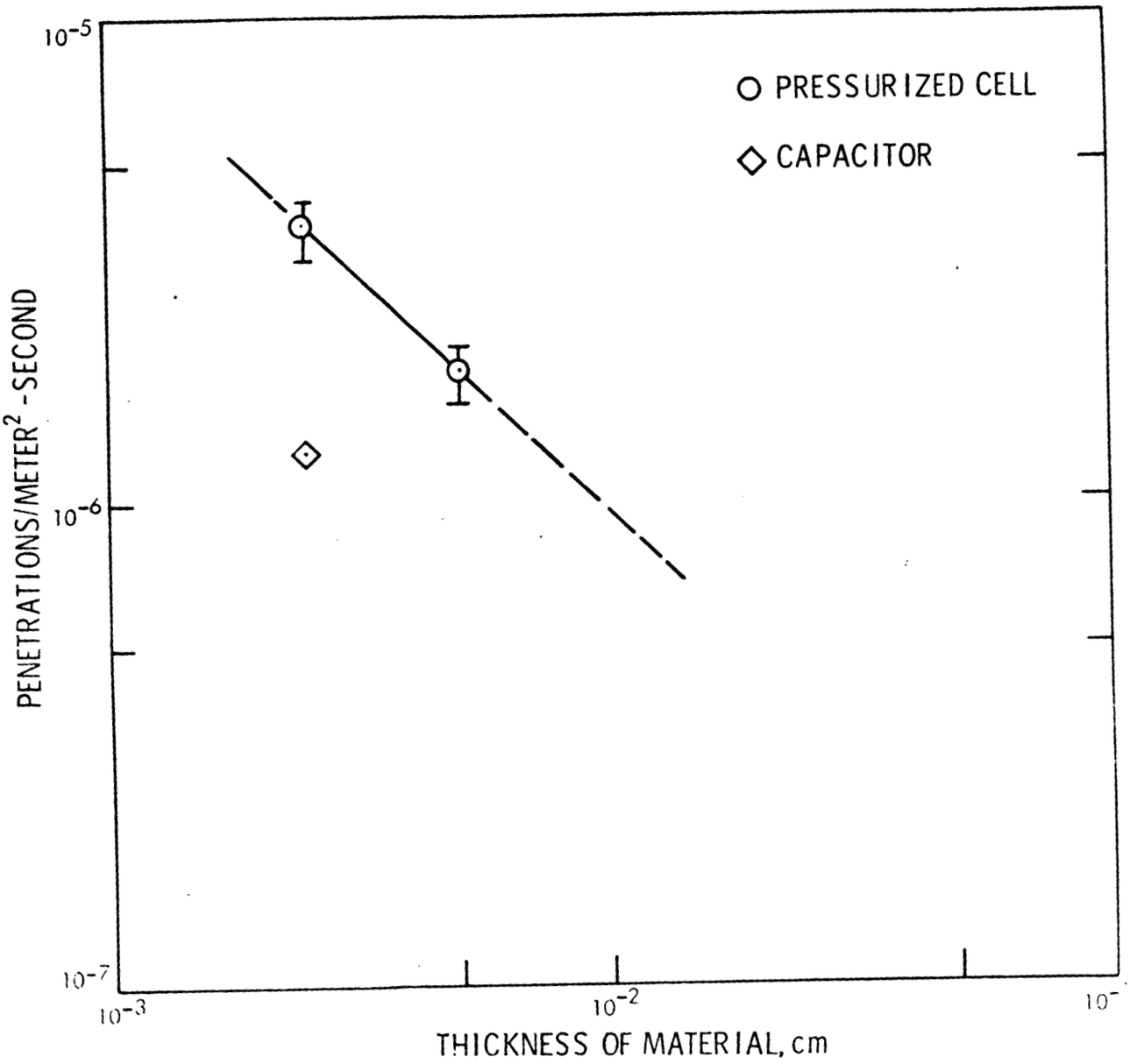
10^-5
10^-6
10^-7
10^-3
10^-2
PENETRATIONS/METER^2 - SECOND
THICKNESS OF MATERIAL, cm
PRESSURIZED CELL
CAPACITOR

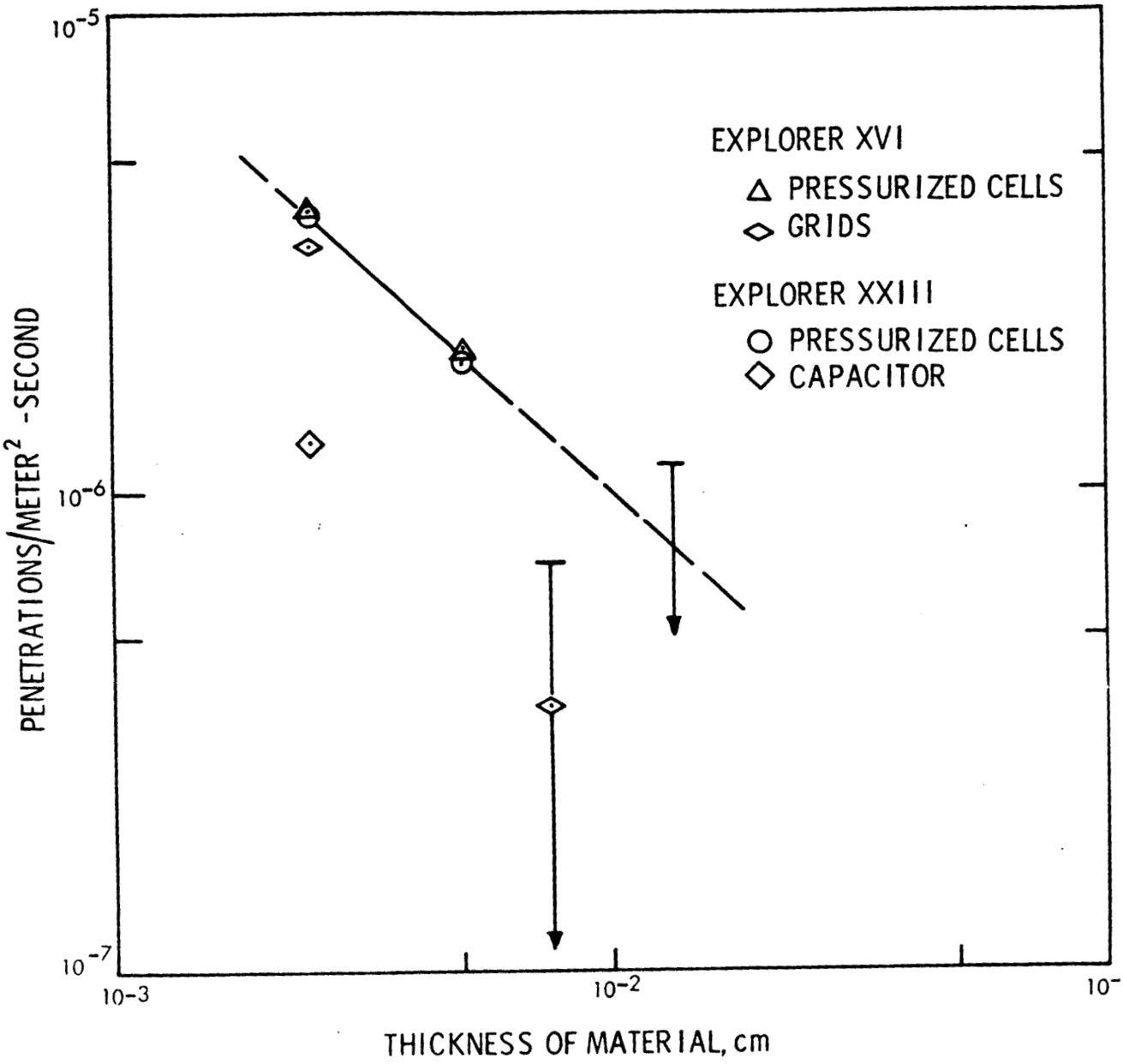
EXPLORER XVI
PRESSURIZED CELLS
GRIDS
EXPLORER XXIII
PRESSURIZED CELLS
CAPACITOR
PENETRATIONS/METER² -SECOND
10⁻⁵
10⁻⁶
10⁻⁷
10-3
10⁻²
10⁻¹
THICKNESS OF MATERIAL, cm

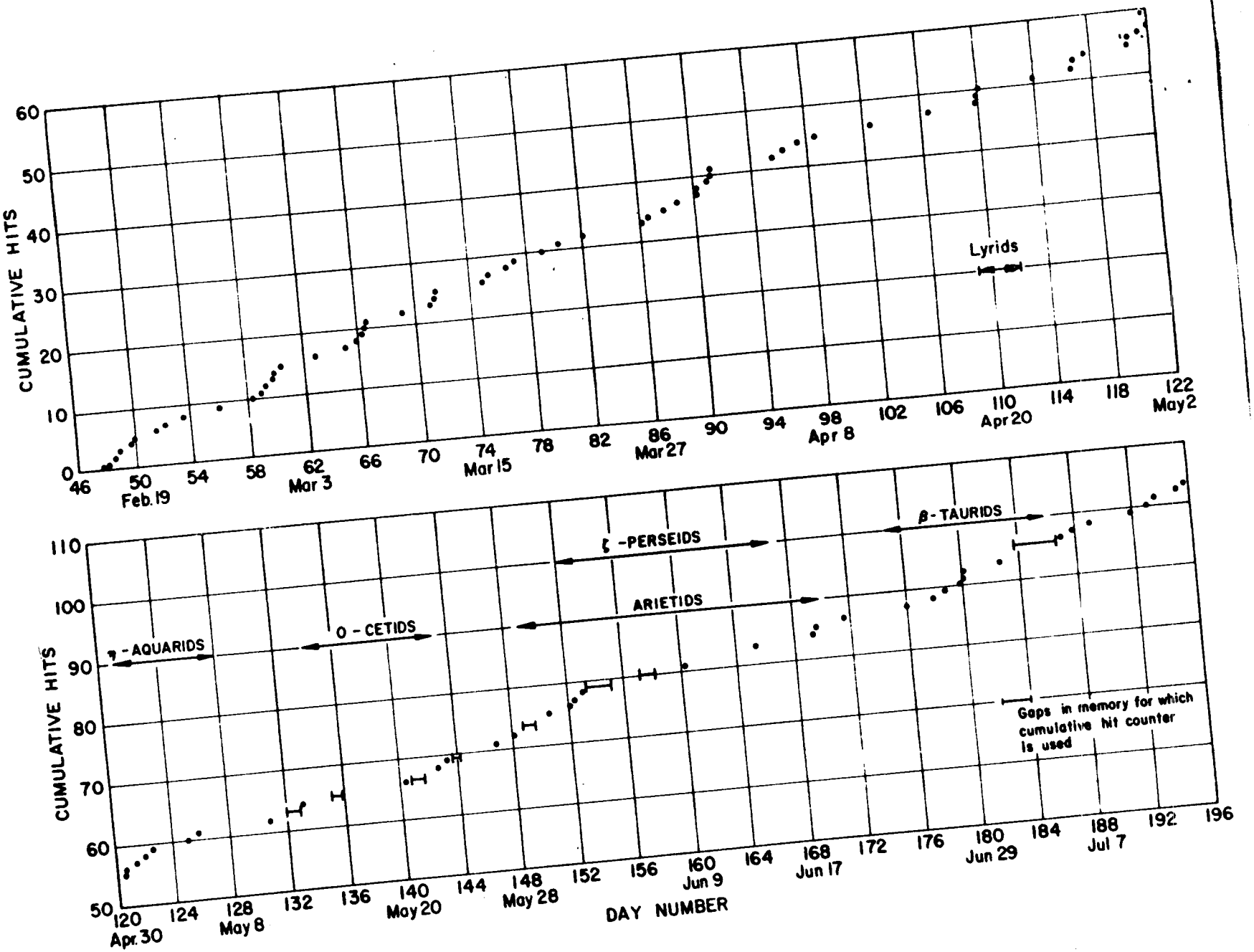
CUMULATIVE HITS
0
10
20
30
40
50
60
Lyrids
46
50
Feb. 19
54
58
62
Mar 3
66
70
74
Mar 15
78
82
86
Mar 27
90
94
98
Apr 8
102
106
110
Apr 20
114
118
122
May 2
CUMULATIVE HITS
50
60
70
80
90
100
110
η - AQUARIDS
O - CETIDS
ζ - PERSEIDS
ARIETIDS
β - TAURIDS
Gaps in memory for which cumulative hit counter is used
120
Apr. 30
124
128
May 8
132
136
140
May 20
144
148
May 28
152
156
160
Jun 9
164
168
Jun 17
172
176
180
Jun 29
184
188
Jul 7
192
196
DAY NUMBER

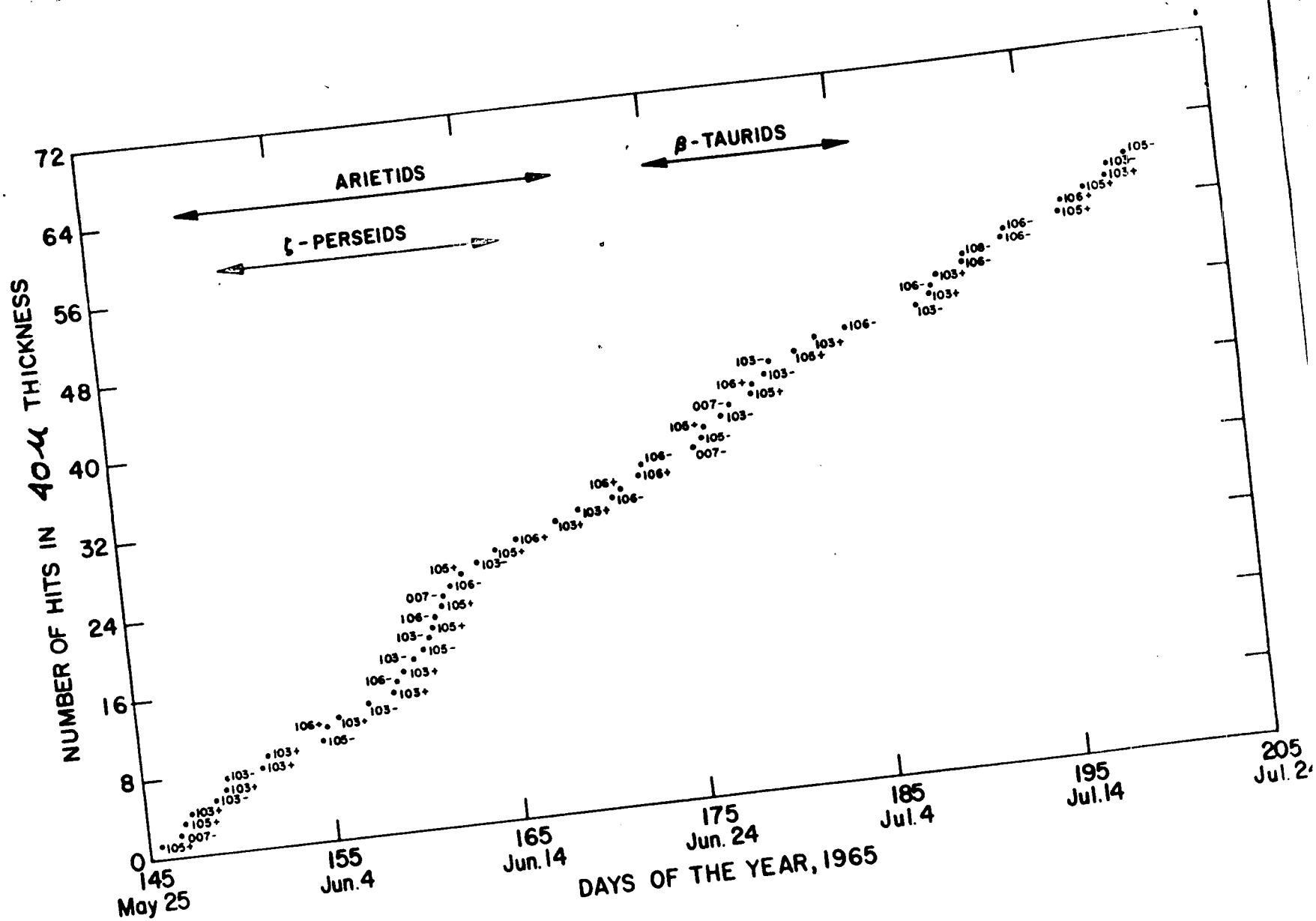
ARIETIDS
ζ-PERSEIDS
β-TAURIDS
NUMBER OF HITS IN 40μ THICKNESS
0
8
16
24
32
40
48
56
64
72
145
May 25
155
Jun. 4
165
Jun. 14
175
Jun. 24
185
Jul. 4
195
Jul. 14
205
Jul. 24
DAYS OF THE YEAR, 1965

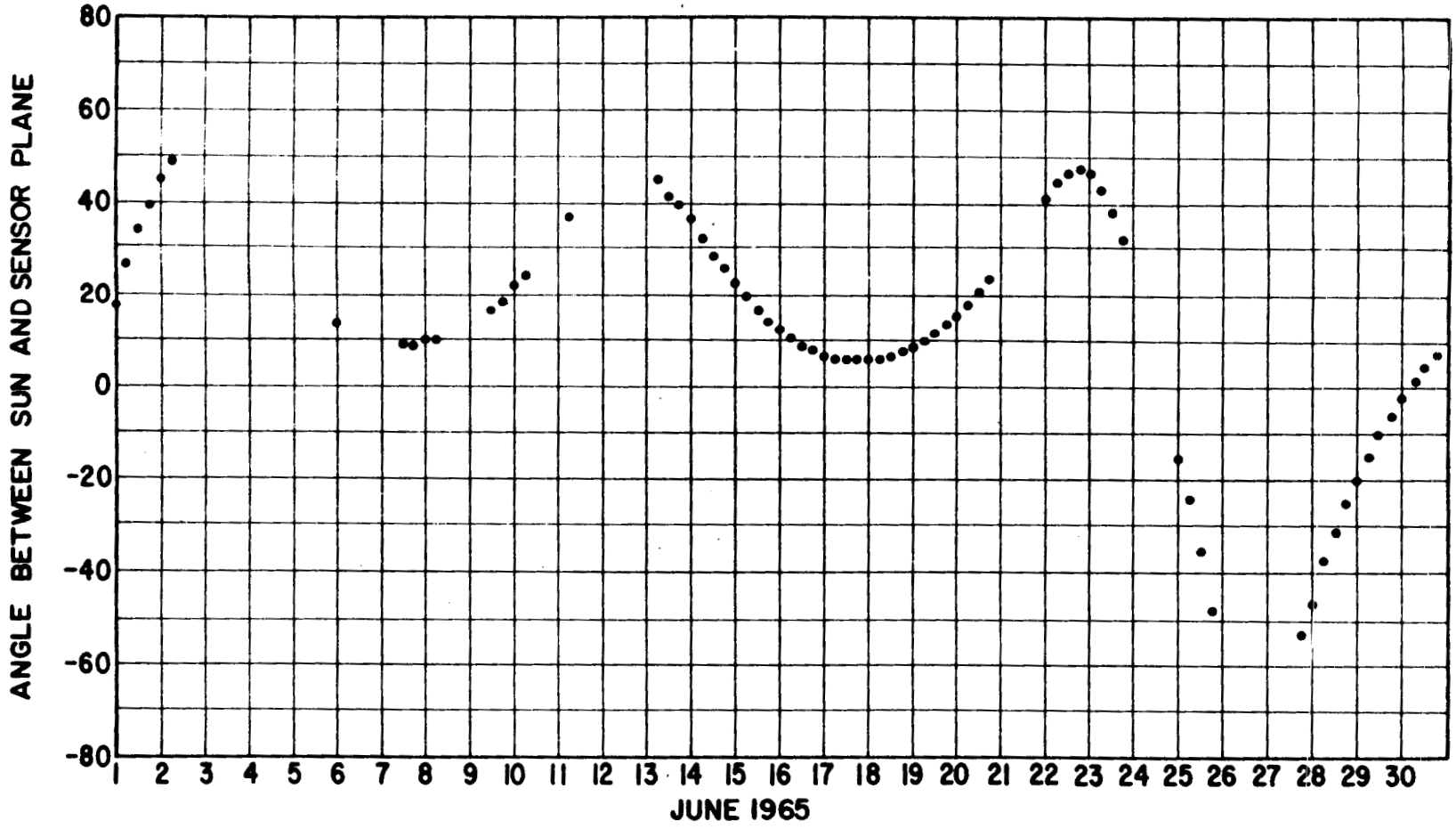
ANGLE BETWEEN SUN AND SENSOR PLANE
80
60
40
20
0
-20
-40
-60
-80
1 2 3 4 5 6 7 8 9 10 11 12 13 14 15 16 17 18 19 20 21 22 23 24 25 26 27 28 29 30
JUNE 1965

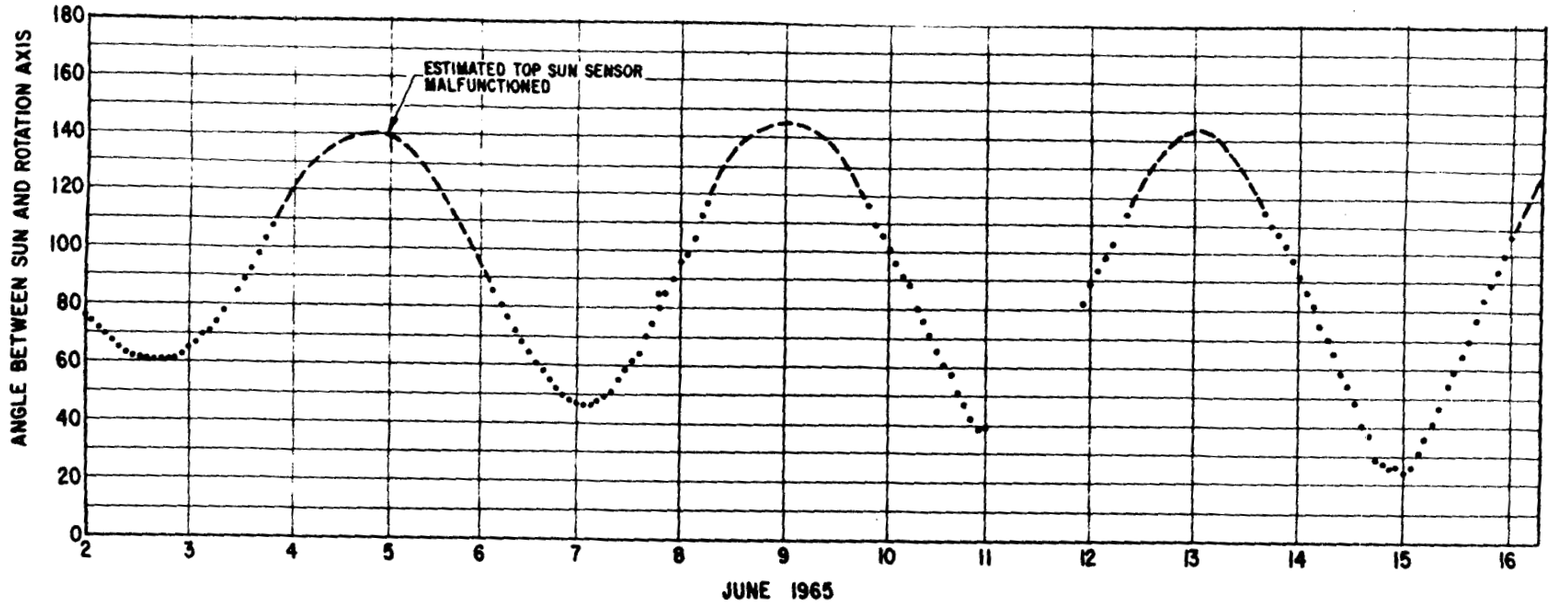
ANGLE BETWEEN SUN AND ROTATION AXIS
180
160
140
120
100
80
60
40
20
0
ESTIMATED TOP SUN SENSOR MALFUNCTIONED
2
3
4
5
6
7
8
9
10
11
12
13
14
15
16
JUNE 1965

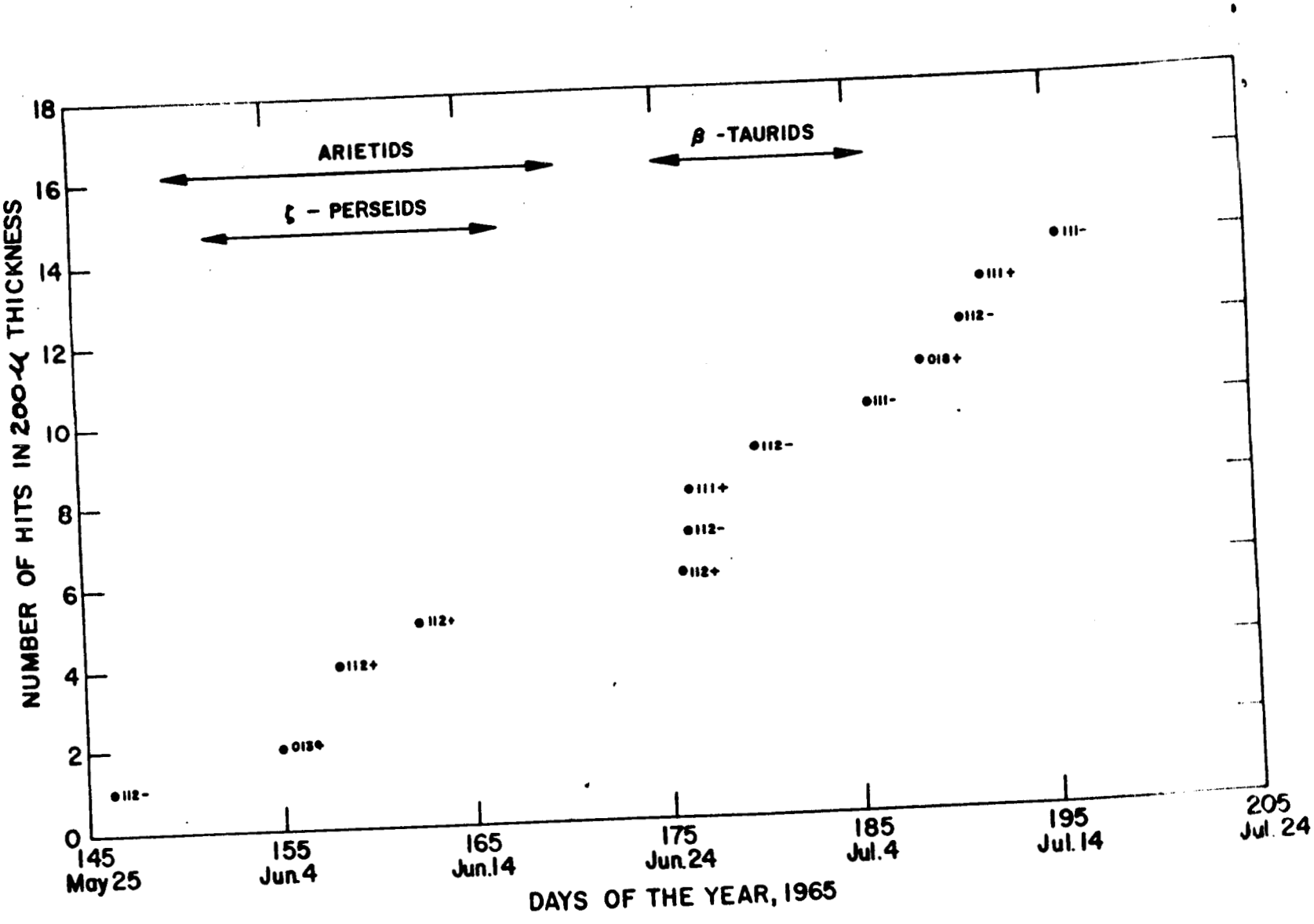
ARIETIDS
ζ - PERSEIDS
β -TAURIDS
NUMBER OF HITS IN 200μ THICKNESS
DAYS OF THE YEAR, 1965
0
2
4
6
8
10
12
14
16
18
145
May 25
155
Jun. 4
165
Jun. 14
175
Jun. 24
185
Jul. 4
195
Jul. 14
205
Jul. 24
●112-
●013+
●112+
●112+
●111+
●112-
●112+
●112-
●111-
●018+
●111+
●111-

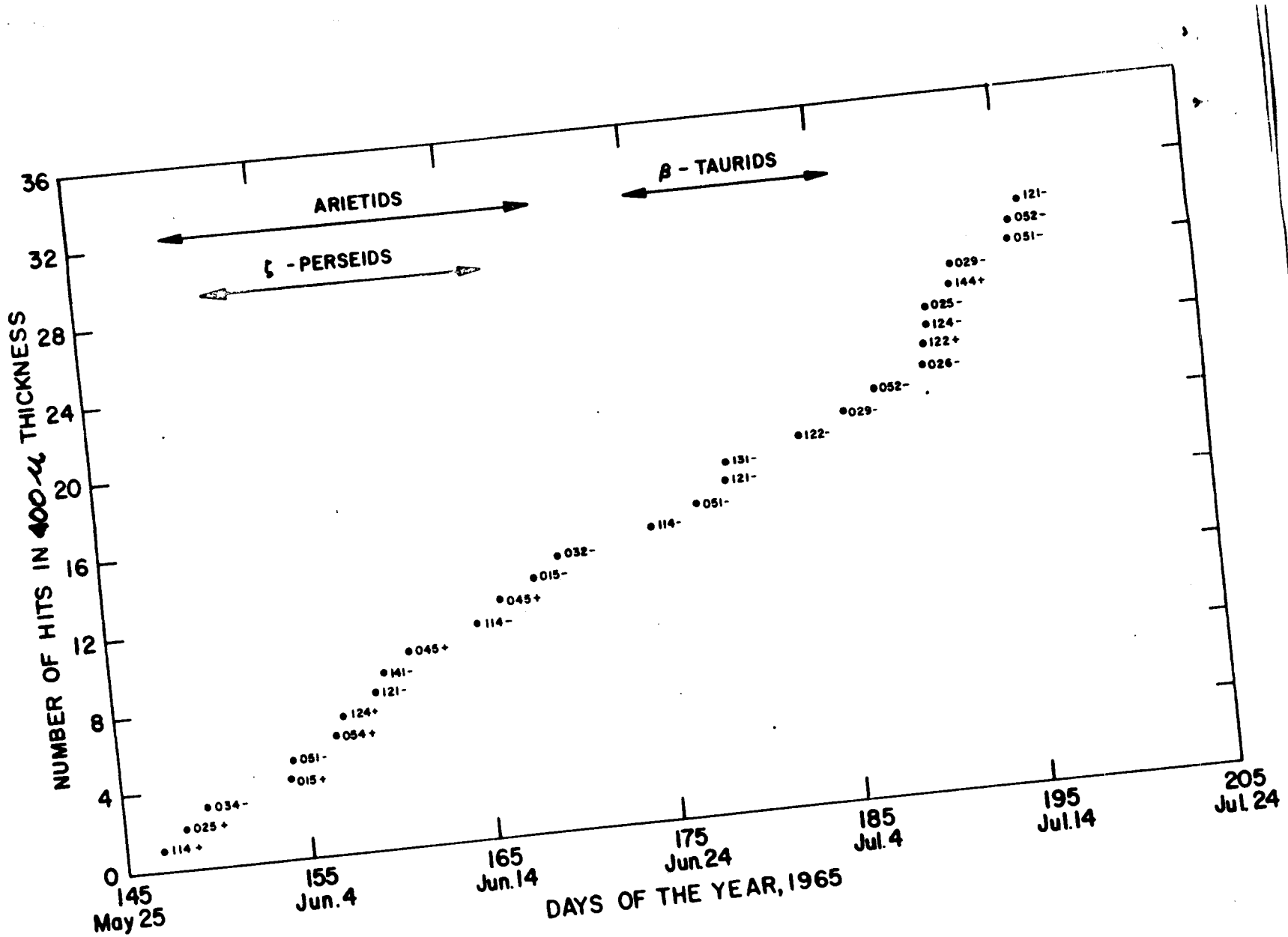
ARIETIDS
ζ - PERSEIDS
β - TAURIDS
NUMBER OF HITS IN 400 μ THICKNESS
0
4
8
12
16
20
24
28
32
36
145
May 25
155
Jun. 4
165
Jun. 14
175
Jun. 24
185
Jul. 4
195
Jul. 14
205
Jul. 24
DAYS OF THE YEAR, 1965
034-
025+
114+
051-
015+
124+
054+
141-
121-
045+
114-
032-
015-
045+
114-
131-
121-
051-
122-
029-
052-
025-
124-
122+
026-
121-
052-
051-
029-
144+

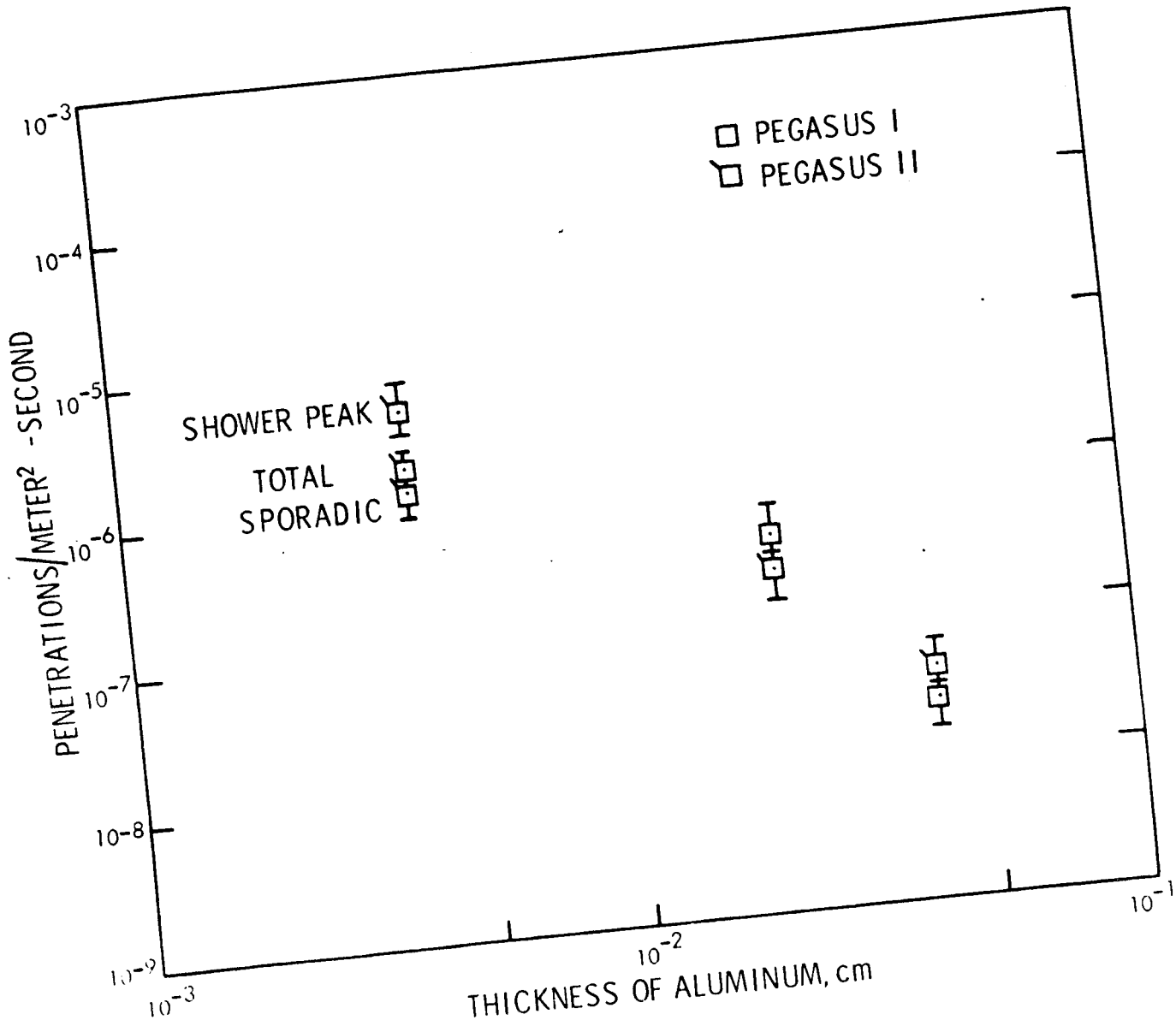
PEGASUS I
PEGASUS II
SHOWER PEAK
TOTAL
SPORADIC
PENETRATIONS/METER² -SECOND
THICKNESS OF ALUMINUM, cm
10⁻³
10⁻⁴
10⁻⁵
10⁻⁶
10⁻⁷
10⁻⁸
10⁻²
10⁻¹

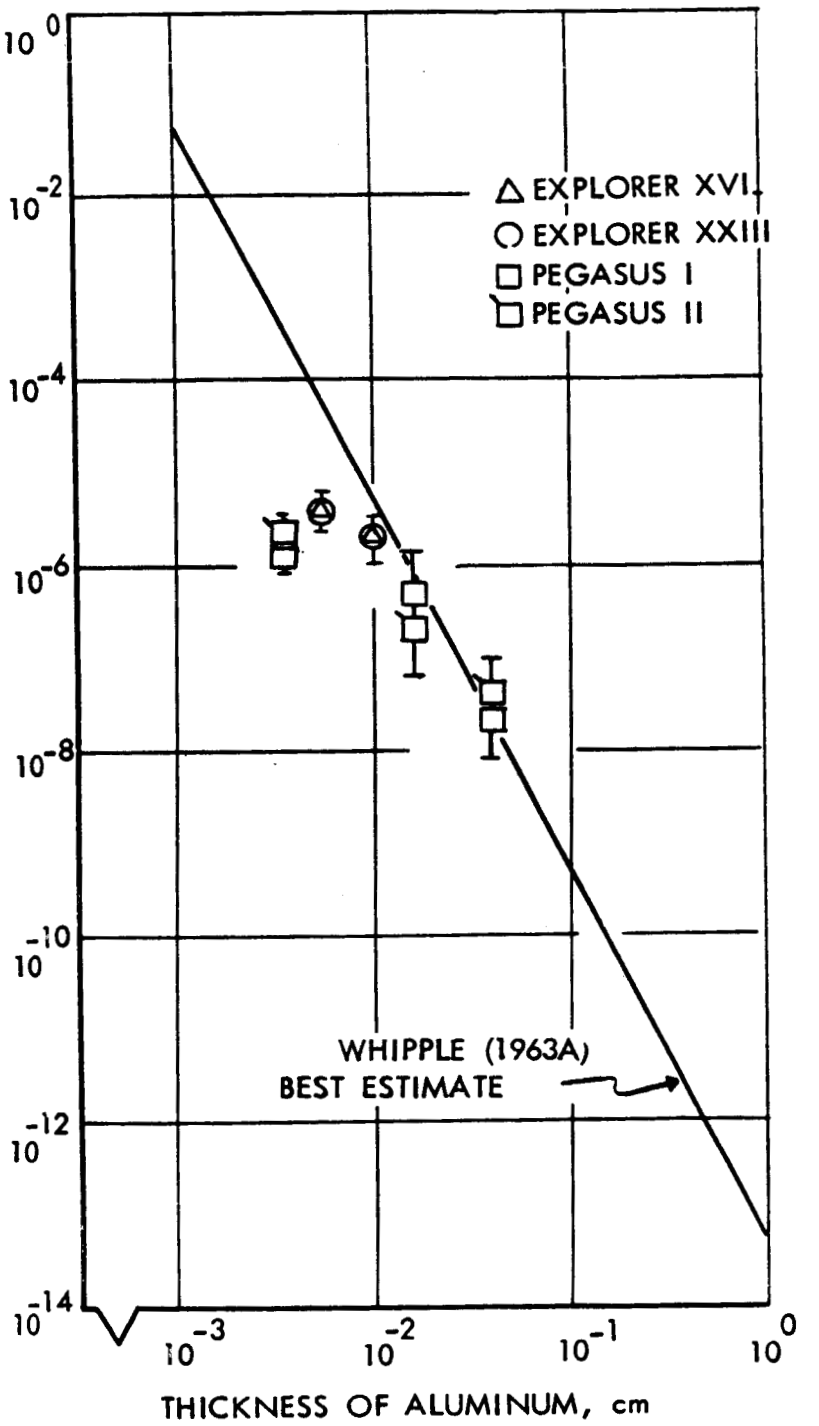

NASA RV65-15599
Rev. 8-5-65